ANL-76-19

ANALYTICAL INVESTIGATION OF CERTAIN ASPECTS OF LMFBR SUBASSEMBLY-FAILURE PROPAGATION

by

W. W. Marr, P. Y. Wang, B. Misra,
A. Padilla, and R. M. Crawford

BASE TECHNOLOGY

UNC-AUA-USERDA

ARGONNE NATIONAL LABORATORY, ARGONNE, ILLINOIS

Prepared for the U. S. ENERGY RESEARCH
AND DEVELOPMENT ADMINISTRATION
under Contract W-31-109-Eng-38

Printed in the United States of America
Available from
National Technical Information Service
U. S. Department of Commerce
5285 Port Royal Road
Springfield, Virginia 22161
Price: Printed Copy $4.00; Microfiche $2.25

Distribution Category:
LMFBR Safety (UC-79p)

ANL-76-19

ARGONNE NATIONAL LABORATORY
9700 South Cass Avenue
Argonne, Illinois 60439

ANALYTICAL INVESTIGATION OF CERTAIN ASPECTS OF LMFBR SUBASSEMBLY-FAILURE PROPAGATION

by

W. W. Marr, P. Y. Wang, B. Misra,*
A. Padilla,** and R. M. Crawford†

Reactor Analysis and Safety Division

February 1976

*Components Technology Division, ANL
**Now at Hanford Engineering Development Laboratory
†Now at Sargent and Lundy, Engineers, Chicago

TABLE OF CONTENTS

LIST OF FIGURES

LIST OF FIGURES

LIST OF FIGURES

LIST OF TABLES

ANALYTICAL INVESTIGATION OF CERTAIN ASPECTS OF LMFBR SUBASSEMBLY-FAILURE PROPAGATION

by

W. W. Marr, P. Y. Wang, B. Misra,
A. Padilla, and R. M. Crawford

ABSTRACT

This report presents the analytical investigation of certain problems in the area of subassembly-to-subassembly failure propagation in LMFBR's. Existing analyses of the response of the adjacent subassembly duct to mechanical loads are reviewed and summarized, and major uncertainties are identified. Additional analyses of the response of the adjacent subassembly to certain thermal loads are presented in two parts. In the first part, the effect of an external heat flux on duct melting and thermal stresses is considered. The external heat fluxes required to produce duct melting or excessive thermal stresses are compared with the heat fluxes that might be expected from the molten fuel deposited on the duct wall. In the second part, a thermal-hydraulic study is performed to investigate the effect of the external heat flux on the coolant temperature distribution in the adjacent subassembly. Both normal subassembly geometry and distorted subassembly geometry are considered. A detailed model of the coolant region formed by the heated duct wall and the displaced fuel pins is also analyzed to determine whether there are severe temperature gradients.

I. INTRODUCTION

This report reviews and summarizes existing work and presents the results of additional analyses of potential or hypothetical mechanisms for subassembly-to-subassembly failure propagation. This report is the third in the series to evaluate the problem of fuel-failure propagation in LMFBR's. In the first report on local initiating events,[1] it was concluded that pin-to-pin failure-propagation modes resulting from postulated initial faults were inherently self-limiting. In the second report,[2] several accident situations were postulated to determine the capability of the accident subassembly duct to withstand severe mechanical and thermal loads. It was found that duct integrity would not be threatened for the expected loads, while severe hypothetical

accidents would likely result in duct failure; in addition, the consequences of a localized failure of the subassembly duct were investigated.

In this report, several modes of propagation for subassembly-to-subassembly failure are identified with the use of safety-assurance diagrams.[3] Certain initiating events and failure-propagation modes that might lead to sustained coolant voiding and subsequent meltdown of subassemblies adjacent to an accident subassembly and beyond are also examined.

This report does not cover the total problem of subassembly-to-subassembly failure propagation. For example, it does not address the problem of combined thermal and mechanical loadings and possible damage to the adjacent control or fuel subassemblies; nor does it consider the sequence of events leading to or following an accident situation postulated in the analysis. However, it does consider parametrically the effect of thermal loading on the duct wall and coolant in the adjacent subassemblies. When relevant initiating accidents are identified and the resulting loadings on the adjacent subassemblies determined, the possibility of subassembly failure propagation can then be assessed using the results presented in this report.

II. INITIAL FAULTS AND THEIR CONSEQUENCES

A previous report on pin-to-pin failure propagation[1] identified initial faults and assessed their potential consequences by fault-tree analysis and accident-progression diagrams. That assessment will not be repeated in this report, but a few significant conclusions of that work will be reviewed. The initial faults were represented in the earlier report by three main categories: (1) random fuel-pin failure, (2) operation with fuel pins under overpower conditions, and (3) debris in the primary coolant system. These postulated initial faults may result in the following potential propagation modes for failure: (1) release of fission gas, (2) chemical reaction between fuel and sodium during continued operation, (3) initial pressure transients due to the vaporization of coolant contacting small amounts of molten materials, (4) blockage of the coolant flow in the subassembly by fuel debris, and (5) localized coolant boiling. These events are summarized in Fig. 1. Detailed analyses were completed for each of these potential problems. On the basis of these analyses, as well as the available experimental results, it was concluded that rapid failure propagation would not occur at low values of fuel burnup and under normal operating conditions. In fact, these modes of failure propagation appeared to be inherently self-limiting.

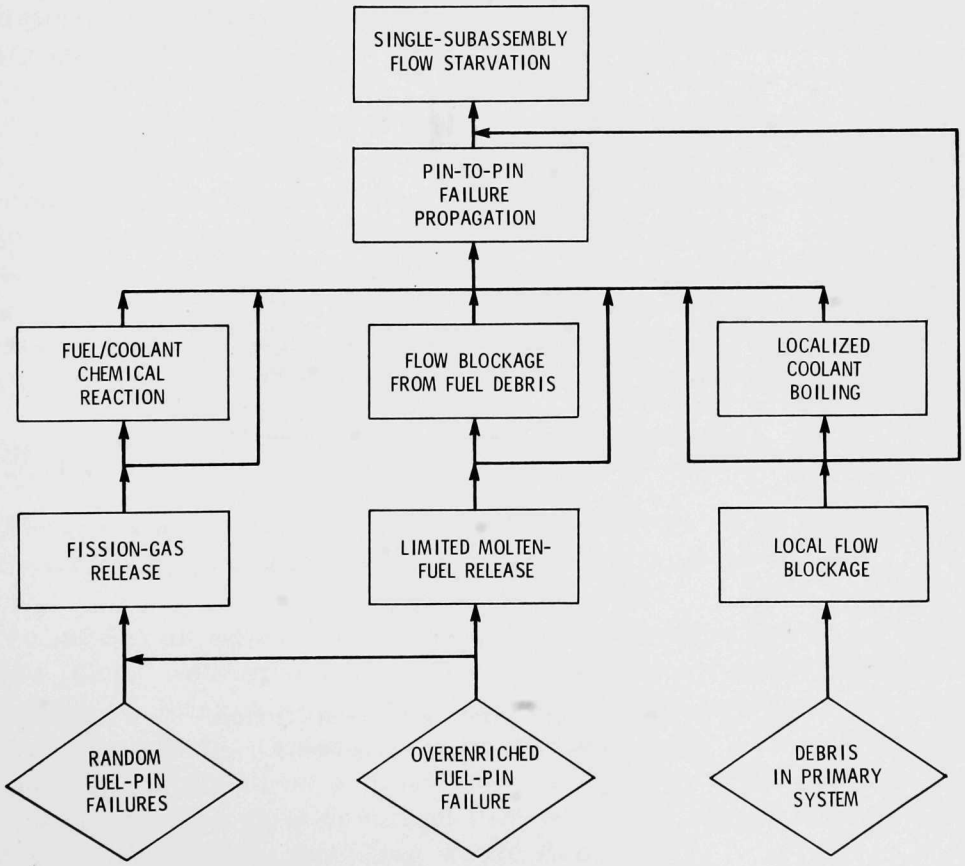

Fig. 1. Potential Initial Faults and Failure-propagation Modes. ANL Neg. No. 900-2179 Rev. 1.

In spite of these results, the integrity of the accident-subassembly boundary was investigated for certain postulated accident situations.[2] It was concluded that a breach of the integrity of the subassembly boundary is not expected to occur for the expected accident sources. However, a breach of the subassembly-boundary integrity might occur for some severe hypothetical accident sources.

This report investigates the integrity of fuel subassemblies adjacent to an accident subassembly. Figure 2 shows the potential modes of subassembly failure propagation. This report does not focus on a specific initiating accident from those identified by the safety-assurance diagrams;[3] instead, parametric studies are made over a range of potential accident conditions. Thus, the results in this report can be used to evaluate the consequences of a number of given accidents that fall within the envelope covered.

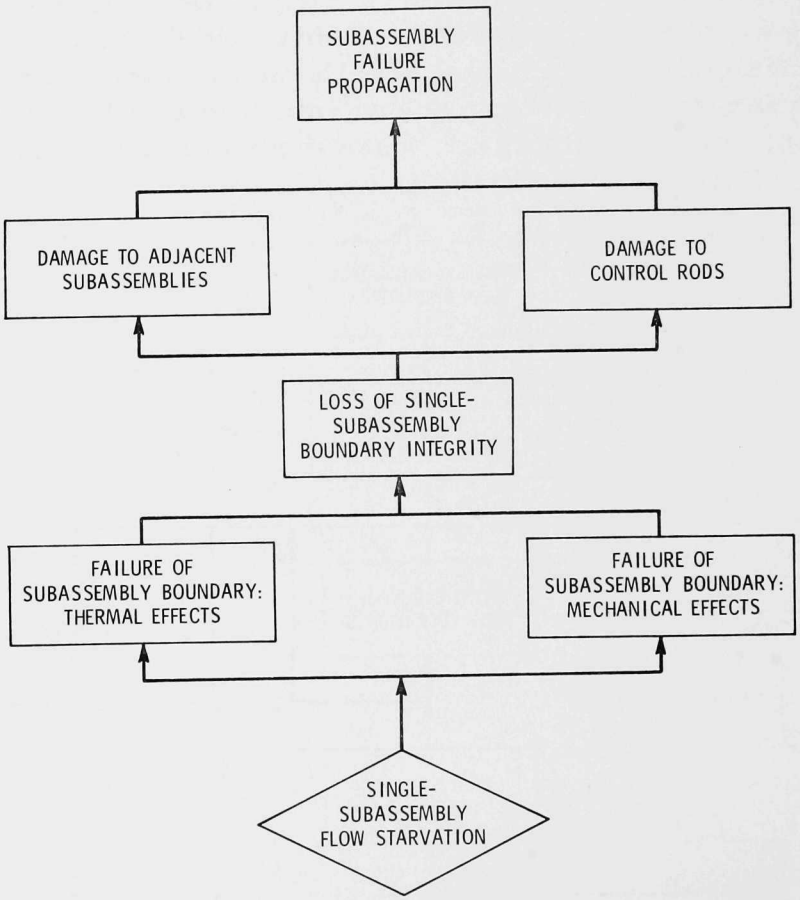

Fig. 2. Potential Modes of Subassembly-failure Propagation. ANL Neg. No. 900-2173 Rev. 1.

III. ANALYSIS OF POSTULATED MODES OF FAILURE PROPAGATION

From the previous discussion of initiating faults, areas of concern in subassembly-to-subassembly failure propagation can be grouped into several modes: (1) the response of the adjacent subassembly to strictly mechanical loads, (2) the response of the adjacent subassembly to strictly thermal loads, and (3) the response of the adjacent subassembly to combined thermal and mechanical loads. Few analytical investigations to predict the capability of an adjacent subassembly duct to withstand external mechanical loadings have been documented. No new analyses have been undertaken for this report, but the limited number of existing analytical studies have been reviewed and are summarized in Sec. A below.

The thermal loading of the adjacent subassembly is considered in two parts: (1) the effect on the duct wall and (2) the effect on the coolant temperature and flow distribution within the fuel bundle. A high external heat flux to the duct wall can result in duct melting and/or excessive thermal stresses which might lead to large deformations or failure. In Sec. B, the heat flux that results in duct melting will be compared with a range of heat fluxes that might be expected from the neighboring accident subassembly. Also, a simplified thermal-stress-analysis model is developed in order to predict the elastic-plastic behavior of the adjacent subassembly duct when it is subjected to a severe temperature gradient.

The coolant temperature and flow distribution in the fuel bundle of an adjacent subassembly are investigated in Sec. C for both normal and distorted subassembly geometries, with and without an external heat flux over the subassembly duct. The purpose of these studies is to see if rapid failure propagation caused by coolant voiding in the adjacent subassembly is possible. Investigation of cases for the distorted subassembly geometry consists of (1) progressively deforming all six flats of an adjacent subassembly inward until three rows of fuel pins are compressed and (2) deforming only one flat inward.

A. Mechanical Loading of Adjacent Subassembly Duct Wall

Previous analytical studies on the response of an adjacent subassembly duct to an external pressure pulse are summarized here.

To model an adjacent subassembly duct subjected to an external pressure pulse, Cole[4] assumed a simply supported beam under uniform lateral static loading to determine the longitudinal elastic bending. The equations for the moments and deflections can be found in Ref. 5. The energy absorbed by the duct was assumed to be a function of the length of the loading zone and the load intensity. It was also assumed that when the stress developed in the duct reached the yield stress, buckling would occur.

Cole later extended his analysis by considering a uniformly distributed load applied to one flat of the subassembly duct supported at the two corners

of the opposite flat.[6] By assuming an elastic-perfectly-plastic stress-strain relationship for the subassembly duct material, he used a limit-load analysis to determine the critical static loadings required to form plastic hinges in the subassembly duct.

Cole performed a parametric study for various cross-sectional dimensions and yield stresses of the duct. He presented a "severe" case in which he assumed that one flat of the subassembly was externally loaded by an energy density of 18.8 in.-lb_f/in.^{2} and that 20% of this energy was absorbed by the duct wall. The following parameters were used: duct dimensions of 4.615 in. across outside flats, 0.14-in. duct-wall thickness, and yield stresses of 14,000 psi and 34,000 psi representing the beginning of life and end of life, respectively, for Type 304 stainless steel at 1000°F. At the beginning of life, the absorbed energy density corresponded to a pressure of 58 psi acting on one flat of the subassembly duct; a deflection of 0.119 in. and a strain of 0.377% resulted. At the end of life, the corresponding pressure was 110 psi, which resulted in a deflection of 0.056 in. and a strain of 0.24%. Failure of the subassembly duct was not expected in either case.

Pan[7] analyzed three different types of external loadings acting on the adjacent subassembly duct: longitudinal uniform pressure, ring load with uniform intensity, and lateral concentrated or distributed loading on one flat of the duct. Assuming an elastic-perfectly-plastic stress-strain relationship for the duct material as well as yield stresses of both irradiated and unirradiated material, he used a plastic limit-load approach through the introduction of plastic hinges at the corners and center of the flats to obtain the critical static external loads (both uniform pressures and ring loadings) for two different duct dimensions. For example, for a duct-wall thickness of 0.151 in., distance of 5.151 in. across outside flats, and yield stress of 40,000 psi (unirradiated material), the uniform external pressure on all six flats required to initiate yielding at the corners of the flats was 220 psi. Higher pressures of 330 and 434 psi were required to form plastic hinges at the corners and at both corners and centers of the duct flats, respectively.

The critical lateral concentrated force on one flat of the adjacent subassembly duct was assumed to arise from contact with the accident subassembly and occurred when plastic hinges around the adjacent subassembly duct were formed. The total deflection of the adjacent subassembly duct due to lateral loading was assumed to be the linear sum of the cross-sectional distortion and the gross (longitudinal) bending deformation.

Coffield and Wattelet[8] used the FEATS finite-element computer code[9] to analyze the deformation of an irradiated subassembly duct (duct-wall thickness of 0.12 in. and across-outside-flats distance of 4.575 in.) subjected to a uniform static external pressure on all six flats. A bilinear stress-strain relationship was used for the duct material, and the following material property parameters, corresponding to a neutron fluence of 2×10^{23} n/cm^2, were

assumed: 75,000-psi yield stress and 2.5% rupture strain at 1000°F, and 30,000-psi yield stress and 0.5% rupture strain at 1500°F. The calculations indicated that the duct was capable of withstanding a uniform external pressure of 1000 psi at 1000°F and 400 psi at 1500°F without reaching the maximum allowable strain. The above analyses are summarized in Table I.

TABLE I. Summary of Analyses of External Loading on Subassembly Duct

Reference	Assumptions	Pressure Loading, psi	Duct Geometry: d = cross-flat outside diameter, in. h = wall thickness, in.	Yield Stress, σ_y, psi	Temp, °F	Results	Remarks
4(GE)	1. Lateral static loading 2. Elastic beam analysis 3. Simply supported	Pressure intensity varies with different loaded length.	d = 4.615 h = 0.14	10,000 50,000		A parametric study for subassembly-duct deflections.	Assuming buckling when reaching yield strength.
6(GE)	1. Static lateral pressure 2. Elastic-perfectly plastic material 3. Limit-load approach 4. HEXDOUT computer program	a. 58 b. 110	d = 4.615 h = 0.14	SS304 a. 14,000 (beginning of life) b. 34,000 (end of life)	1000	a. Deflection = 0.119 in. Strain = 0.377% b. Deflection = 0.056 in. Strain = 0.24%	No failure expected for either case. Parametric study also performed for different duct dimensions and yield stresses.
7(AI)	1. Static uniform pressure 2. Elastic-perfectly plastic material 3. Limit-load approach	a. 220 b. 330 c. 434	d = 5.151 h = 0.151	40,000		a. Yielding at flat corners b. Plastic hinges at flat corners c. Plastic hinges at flat center and corners	Ring loading and concentrated load with other duct dimension and yield stress values also considered.
8(WARD)	1. Static uniform pressure 2. Elastic-plastic with hardening 3. FEATS finite-element computer code	a. 1000 b. 400	d = 4.575 h = 0.12	SS316 at fluence of 2×10^{23} n/cm^2 a. 75,000 (rupture strain = 2.5%) b. 30,000 (rupture strain = 0.5%)	a. 1000 b. 1500	a. Max deflection < 0.05 in. b. Max deflection < 0.05 in.	In both cases, the values of rupture strain were not reached.

The above summaries of previous analyses indicate that there are large differences in the results obtained from the various approaches. These differences are due not only to the different parameters (geometry, material property, and loading), but also to the fact that different assumptions were made. Cole[4,6] and Pan used simplified approaches such as static simulation of the dynamic problem and idealization of the material property (elastic or elastic-perfectly-plastic stress-strain relationships). Coffield and Wattelet[8] circumvented the material-property idealization (but not the static simulation) by using the FEATS computer code. Although they found it necessary to assume a uniform pressure loading on all sides of the duct, they claimed that FEATS can handle plane, two-dimensional problems, which would make it unnecessary to assume such a uniform loading. Furthermore, MPR Associates[10] have indicated that the FEATS code may underestimate strains and deflections for certain axisymmetric elastic-plastic problems.

Based on this assessment of the analyses discussed above, several uncertainties should be resolved in order to obtain a more accurate assessment of the response of the subassembly duct to external mechanical loadings. The following uncertainties are particularly significant:

1. Accurate prediction of the characteristics of the external loading (pulse shape, peak pressure, pulse duration, etc.) is important to the selection of a static or dynamic approach. Most of the analyses discussed above assumed

that the external loadings applied to the duct were static. For certain types of pressure-pulse loadings, dynamic effects may be significant in determining the duct response. If a static approach is taken, it is important to show that it is an adequate approximation.

2. The nonlinearities in the material properties for irradiated and unirradiated ducts should be taken into account. Elastic or elastic-perfectly-plastic idealizations may provide some general trends, but the results may be overly conservative.

3. Instability of the subassembly duct due to buckling of the duct flat may occur before the maximum allowable strain in the duct is attained.

4. The analyses should be compared with experimental results over the range of deflections and strains of interest in order to demonstrate the validity of the analytical model.

5. For asymmetric problems involving cross-sectional distortion and longitudinal deflection of the subassembly duct, a three-dimensional model may yield much more reliable results than two-dimensional models.

6. Proper modeling of the intersubassembly-gap sodium and the subassembly-duct internals may strongly affect the duct response under certain lateral pressure-pulse loadings.

7. Better property data and failure criteria for irradiated materials are needed to improve the confidence in the material parameters used in the analysis.

B. Effect of External Heat Flux on Adjacent Subassembly Duct Wall

In Ref. 1, it was concluded that large amounts of molten fuel are not expected to be generated in an accident subassembly. In this section, the existence of molten fuel is postulated solely in order to predict the response of an adjacent subassembly duct wall under severe thermal-loading conditions.

1. Melting of Duct Wall

Figure 3 shows the fraction of the duct wall melted as a function of the inside surface temperature for various values of external heat flux. This

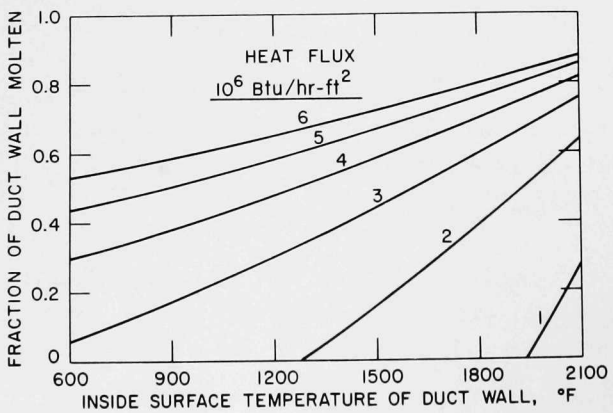

Fig. 3

Effect of External Heat Flux on Melting of Adjacent Subassembly Duct Wall. ANL Neg. No. 900-3644.

figure was obtained by a simple application of Fourier's equation of heat conduction. The inside surface temperature of the duct wall could be substantially greater than the coolant temperature, depending on the value of the sodium-film heat-transfer coefficient and the heat flux. For a heat flux of 1×10^6 Btu/hr-ft^2, no melting of the adjacent subassembly duct wall will occur if the inside-surface temperature can be maintained below ~1900°F. For a heat flux of 2×10^6 Btu/hr-ft^2, the maximum inside-surface temperature to prevent duct melting is ~1300°F. For heat fluxes of 3×10^6 Btu/hr-ft^2 and higher, some degree of duct melting cannot be prevented. The ability of the coolant to maintain the inside surface below these maximum values depends on the efficiency of coolant-mixing mechanisms to remove the heat from the coolant region immediately adjacent to the duct wall and distribute it more uniformly throughout the fuel bundle. It will be shown in Sec. III.C below that the coolant-mixing mechanisms are efficient enough to prevent duct melting for heat fluxes up to about 2×10^6 Btu/hr-ft^2.

Heat fluxes that could be expected from molten fuel deposited on the outside of the subassembly duct are frequently based on the "maximum nonboiling fuel thickness." That is, the radial heat flux transferred to the duct wall is generated in the thickness of fuel that is below the fuel boiling point. Based on heat conduction alone, the thickness of the fuel layer that is at the fuel boiling point at the outer surface and at the duct melting point at the inner surface is about 0.05 in. for full-power conditions and corresponds to a heat flux of about 1.2×10^6 Btu/hr-ft^2. Convection within the liquid portion of the fuel layer may increase the heat flux slightly to about 1.4×10^6 Btu/hr-ft^2. For shutdown conditions, the maximum nonboiling fuel thickness is about five times as thick, but the corresponding heat flux at this reduced power condition is only about 0.4×10^6 Btu/hr-ft^2.

The concept of a nonboiling fuel thickness implies the existence of a core of boiling liquid fuel that condenses at another location of the subassembly. Although condensation heat fluxes of about 4×10^6 Btu/hr-ft^2 are conceivable,[11] it is more probable that fuel vaporization (boiling) would lead to eventual and permanent redistribution of the fuel, with a portion of it outside the active core region. Therefore, the duct wall is not expected to melt, because the maximum heat flux due to molten fuel deposited on the outside of the subassembly duct is about 1.4×10^6 Btu/hr-ft^2 and the duct wall can tolerate heat fluxes up to about 2×10^6 Btu/hr-ft^2 without melting.

2. Thermal-stress Analysis of Duct Wall

Although the duct wall may not melt when molten fuel is deposited on the outside of the subassembly duct, the severe temperature gradient caused by the high heat flux through the duct wall may result in excessive thermal stresses. These thermal stresses could result in an inelastic condition of the duct wall during which large deformations or failure could occur. Hence, it is important to determine when such a condition could be attained. In

order to provide a scoping analysis of this complex problem, assumptions were made for the present analysis as follows:

- The adjacent subassembly duct is subjected to a uniformly distributed high temperature on the outer surface of one flat.
- The temperature gradient through the thickness of the flat is linear.
- The longitudinal variations and end effect are negligible.
- The duct material obeys an elastic-perfectly-plastic, stress-strain relationship.
- The membrane stresses developed in the flat are negligible.

a. Temperature Gradient Only. In Ref. 2, it was postulated that a uniformly distributed high temperature was applied to the inner surface of one flat of the accident subassembly duct, and the temperature-gradient limits that the duct could withstand both elastically and plastically were predicted. That analysis can also be used in the present case in which a uniformly distributed high temperature is postulated to occur on the outer surface of one flat of the adjacent subassembly duct. The analysis will not be repeated here; see Ref. 2 for details.

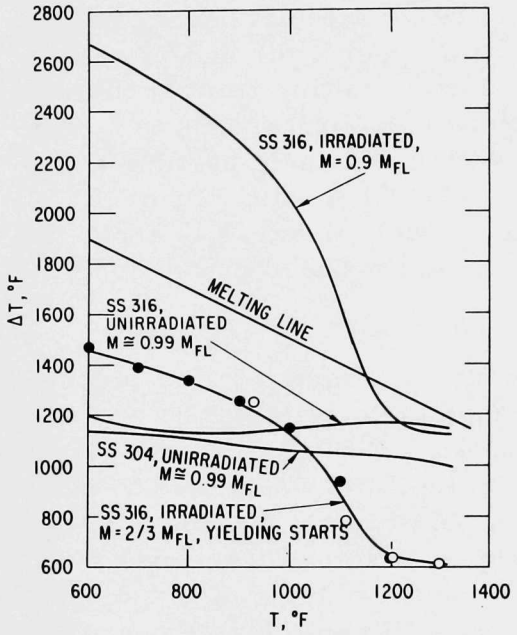

Fig. 4. Effect of Irradiation on Temperature Gradient for Elastic-Plastic Behavior of Subassembly Duct Wall. ANL Neg. No. 900-1820 Rev. 1.

The results are summarized in Fig. 4, which presents the temperature-gradient limits for both irradiated and unirradiated ducts. The "melting line" corresponds to the outer surface being at the melting point and the inner surface at temperature T. For unirradiated ducts, deformation and failure may occur before the duct starts to melt. For irradiated ducts, failure might occur either before or after the duct starts to melt. For example, if the irradiated duct is assumed to have an extremely low ductility, say, ~0.2%, which is thought to be an overly conservative assumption, then it might fail when the bending moment M is two-thirds of the plastic flow moment M_{FL}, which denotes the theoretical ultimate plastic carrying capacity of the duct wall. For this conservative case, the irradiated duct is predicted to fail before the duct melts.

If the irradiated duct is assumed to have more ductility than in the previous case, as experimental data indicate, then failure would not occur

until significant plastic flow of the material is established, say $M = 0.9\, M_{FL}$. For this case, the temperature-gradient limit is much higher, and the duct might melt before failure due to plastic flow. Although the irradiated duct appears to have a higher resistance against thermal loading than the unirradiated annealed duct, its strength depends on temperature, total amount of neutron fluence, ductility, and prestraining. Better data on the properties of irradiated duct materials are needed in order to define appropriate failure criteria adequately. For the present study, the unirradiated material property data were taken from Refs. 12 and 13. The irradiated data were taken from Refs. 14 and 15.

b. Combined Temperature Gradient and Internal Pressure. In this case, the adjacent subassembly duct is subjected to a moderate uniform internal pressure in addition to a high temperature applied along the outer surface of one duct flat. The combined moment at the ends (corners) of this flat due to the interaction of the temperature gradient and the internal pressure increases as the temperature gradient increases, and eventually reaches the elastic limit. The largest temperature gradient, ΔT_y, that a duct is able to withstand elastically can be predicted by

$$\Delta T_y = \frac{60}{19E\alpha}\left(\sigma_y - \frac{pL^2}{2h^2}\right), \qquad (1)$$

where E is the modulus of elasticity, α is the coefficient of thermal expansion, σ_y is the yield stress, p is the internal pressure, h is the duct-wall thickness (0.12 in. for the FFTF subassembly), and L is the flat width (2.641 in. for the FFTF subassembly). The material parameters used in the calculations are assumed to be those at temperature T.

Figure 5 shows the variation of ΔT_y for an unirradiated annealed duct with duct-wall temperatures (inner surface) ranging from 100 to 1300°F and for different values of the internal pressure. Even without a temperature gradient, the annealed duct can exceed the elastic limit if the pressure is sufficiently high (e.g., near the subassembly inlet where the temperatures are low and the pressures are high). The curve for p = 0 shows a slight

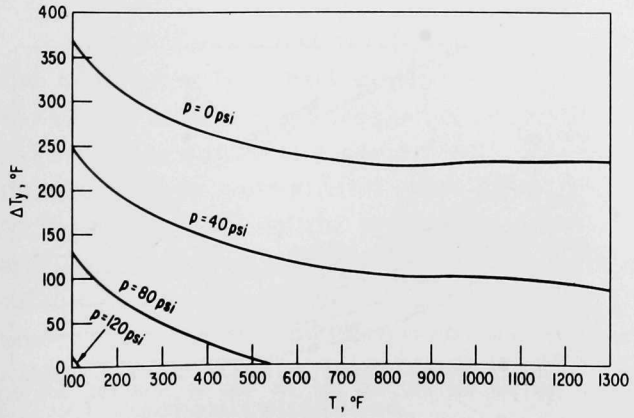

Fig. 5

Temperature-gradient Limits for Elastic Behavior of a Type 316 Stainless Steel Duct Wall of an Unirradiated Subassembly. ANL Neg. No. 900-3606.

increase of ΔT_y for $T \geq 900°F$; this is due to variations in the parameters E and α at various temperatures. This slight temperature perturbation is believed to be of no real significance.

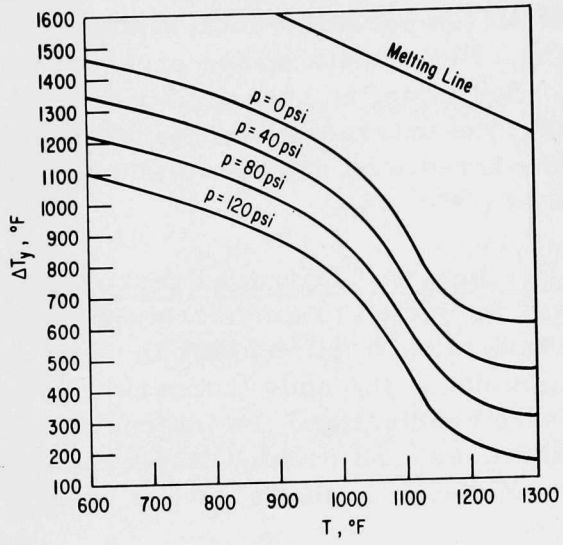

Fig. 6. Temperature-gradient Limits for Elastic Behavior of a Type 316 Stainless Steel Duct Wall of an Irradiated Subassembly. ANL Neg. No. 900-3604.

Figure 6 shows the variation of ΔT_y for an irradiated duct for duct-wall temperatures from 600 to 1300°F for different values of the internal pressure. In this figure, the "melting line," denoting the start of duct melting, is higher than the curves for ΔT_y. Therefore, even for irradiated ducts, the elastic limit will be exceeded before melting of the duct begins. The effect of increasing internal pressure is to decrease the temperature gradient required to reach the elastic limit.

When the temperature gradient increases beyond ΔT_y, the combined moment at the ends of the flat exceeds the elastic limit and reaches the elastic-plastic range. By means of inelastic analysis, the temperature-gradient limit can be approximated by

$$\Delta T = \frac{60}{19E\alpha}\left\{\frac{\sigma_y}{[3(1-\zeta)]^{1/2}} - \frac{pL^2}{2h^2}\right\}, \qquad \Delta T \geq \Delta T_y, \tag{2}$$

where $\zeta = M/M_{FL}$.

Figure 7 shows the temperature-gradient limit ΔT for an unirradiated annealed duct assuming $\zeta \simeq 0.99$. Since all the curves are below the "melting line," significant deformation and failure of the duct may occur before the duct starts to melt. The effect of increasing the internal pressure is to decrease the temperature gradient required for deformation of the duct.

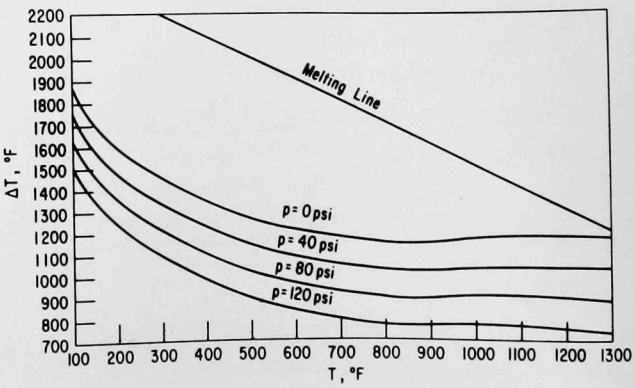

Fig. 7

Temperature-gradient Limits for Plastic Behavior of a Type 316 Annealed Stainless Steel Duct Wall of an Unirradiated Subassembly for $\zeta \simeq 0.99$. ANL Neg. No. 900-3602.

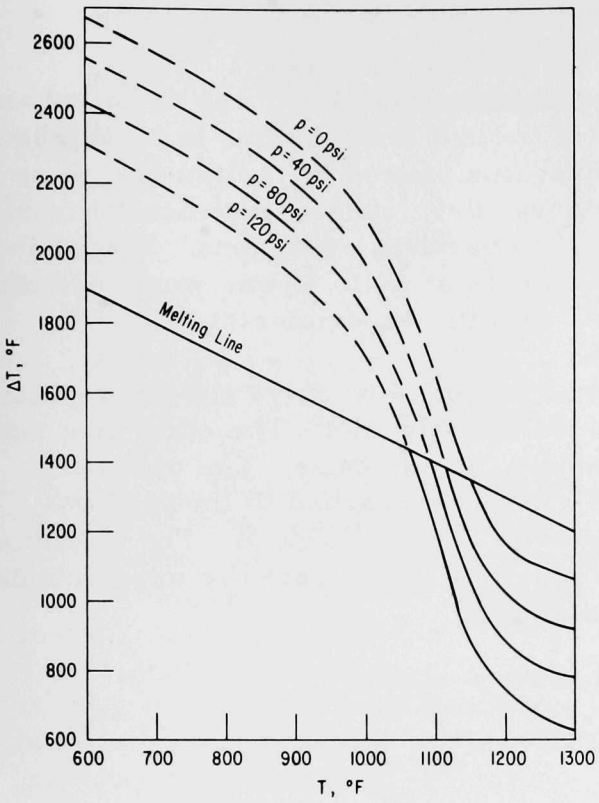

Fig. 8. Temperature-gradient Limits for Plastic Behavior of a Type 316 Stainless Steel Duct Wall of an Irradiated Subassembly for $\zeta = 0.90$. ANL Neg. No. 900-3603 Rev. 1.

Figure 8 shows the temperature-gradient limit ΔT for an irradiated duct assuming that failure (significant deformation) occurs at $\zeta = 0.90$. This criterion is not as conservative as the assumption that failure occurs when yielding starts ($\zeta = 2/3$), but it does not allow as much plastic deformation as was assumed for the unirradiated duct ($\zeta \simeq 0.99$). The curves are above the "melting line" for temperatures less than about 1000°F and below for temperatures greater than about 1200°F. Therefore, it is predicted that at low temperatures the irradiated duct will not significantly deform before melting occurs, and that at higher temperatures the irradiated duct might deform and fail before the start of melting.

From the above analyses, it is concluded that the irradiated adjacent subassembly duct may provide a significantly stronger barrier to prevent failure due to thermal loading than the unirradiated duct. However, since the properties of an irradiated duct are strongly dependent on many factors, such as temperature, total neutron fluence, ductility, and prestraining, an appropriate failure criterion must be adequately defined. Note also that the present analysis only provides a general prediction of the response of a subassembly duct under thermal loadings, and more refined analytical methods and failure criteria are required for detailed calculations.

C. Effect of External Heat Flux on Coolant-temperature Distribution in Fuel Subassembly

The external heat flux due to molten fuel deposited on the outside of the subassembly duct could not only cause melting or excessive thermal stresses in the duct wall, but it could also result in excessive coolant temperatures adjacent to the duct wall. Therefore, a thermal-hydraulic analysis was performed to determine conditions under which the coolant temperatures next to the duct wall might approach the local boiling point. The result of this analysis will be confirmed by appropriate ex-reactor tests.[16] In the first part of the study, the normal subassembly geometry was assumed. In the second part, a more severe situation was investigated in which the subassembly duct and fuel-pin bundle were assumed to be partially deformed as a result of external mechanical forces.

1. Normal Subassembly

The thermal-hydraulic computer code FORCMX[17] was modified and used in the investigation of perturbations of coolant temperature in an adjacent subassembly resulting from an external heat flux caused by molten fuel in an accident subassembly. The FORCMX code was developed at Atomics International as a design tool for predicting LMFBR operating conditions. From the results of the 91-pin coolant-mixing experiments at ANL, it was concluded that the FORCMX predictions agreed quite well with the experimental data.[18,19]

A uniform external heat flux was assumed to cover the entire heated length (36 in.) of one flat of the adjacent subassembly duct. The other five subassembly flats were conservatively assumed to be adiabatic. The operating conditions and geometry used in the calculations correspond to those of the FFTF maximum power subassembly[20] and are listed in Table II. The calculational parameters used in FORCMX were obtained from hydraulic experiments with fuel subassemblies at Atomics International.[21]

TABLE II. Operating Conditions and Geometry for External Heat-flux Analysis; Normal Geometry

Pin OD	0.23 in.
Pin-to-pin triangular pitch	0.286 in.
Heated length	36 in.
Average linear power for fuel pin	10.16 kW/ft
Axial power peaking factor (chopped cosine)	1.24
Radial power peaking factor	1.0
Average inlet mass velocity	4.028×10^6 $lb_m/hr\text{-}ft^2$
Coolant inlet temperature	792°F

Figure 9 shows the layout of the FORCMX coolant subchannel for a 217-pin bundle. The external heat flux is assumed to be uniformly applied to the flat shown at the bottom of the figure (but not including the corner subchannels) along the entire heated length (36 in.). Figure 10 shows the profiles of the across-flats coolant temperature at the top of the heated length under normal operating conditions and with an external heat flux of 4.0×10^6 Btu/hr-ft^2. Only about six rows of coolant subchannels away from the heated duct wall are affected by the external heat flux.

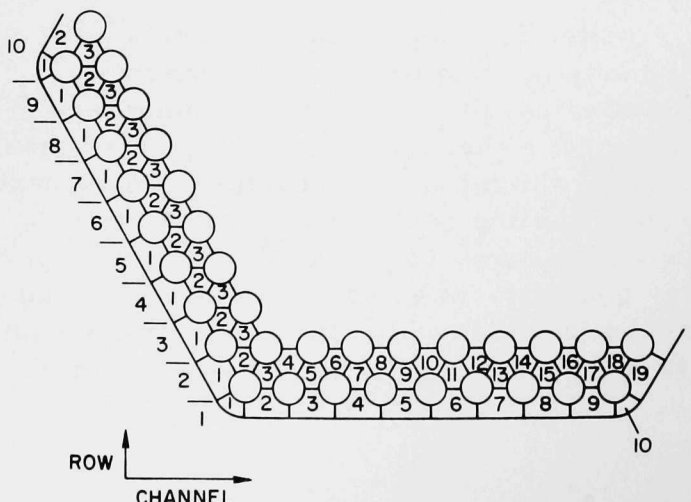

Fig. 9

Layout of FORCMX Coolant Subchannel for a 217-pin Bundle. ANL Neg. No. 900-3636.

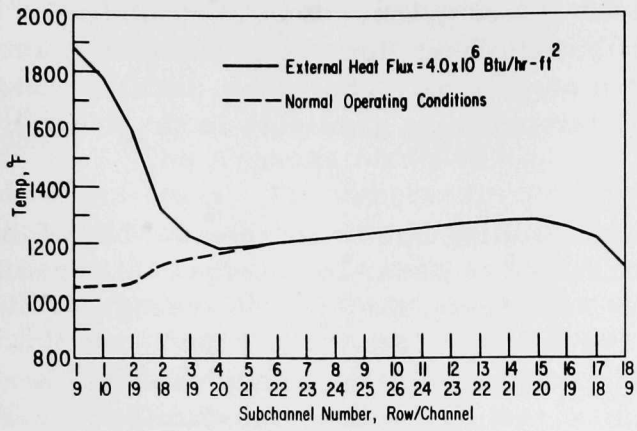

Fig. 10

Across-flats Coolant-temperature Profiles at the Outlet of the 217-pin Bundle. ANL Neg. No. 900-3601 Rev. 1.

Figure 11 shows the maximum coolant temperature (for Row 1, Channel 9 at the top of the heated length) as a function of external heat flux at full-power, full-flow conditions. At normal subassembly pressures, local coolant boiling would be expected to occur between 1800 and 1900°F. Therefore, to produce local coolant boiling, the external heat flux would have to be about 4 x 10^6 Btu/hr-ft^2. For this high heat flux, the subassembly duct wall will be almost three-fourths molten (see Fig. 3).

For more reasonable values of the external heat flux, local coolant boiling is not expected to be a problem. For example, the heat flux based on the maximum nonboiling fuel thickness causes local coolant temperatures of about 1300°F.

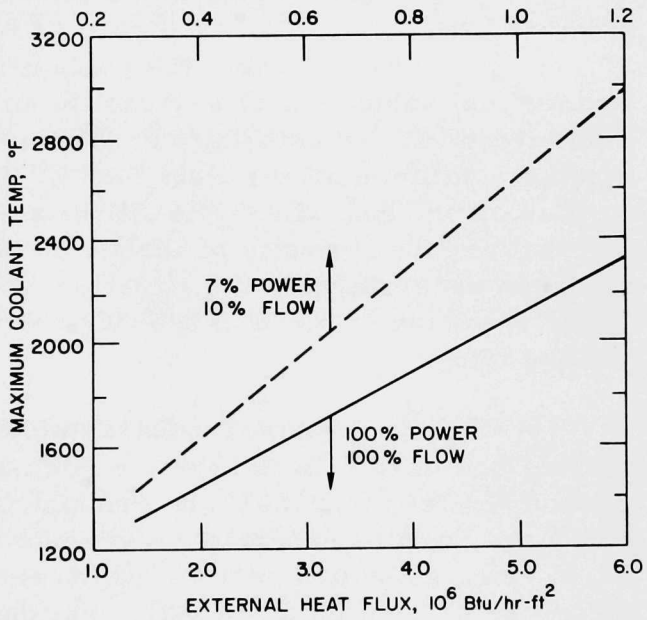

Fig. 11. Maximum Coolant Temperature in the 217-pin Bundle as a Function of External Heat Flux. ANL Neg. No. 900-3637.

Reactor-shutdown conditions were also investigated. Immediately following a scram, the reactor power decays to 10-15% of its normal value while the flow is still relatively high. After 30-40 sec, the power decreases to 5% and the flow to about 10%.[22] Since the power-to-flow ratio during the transient immediately following the scram is small, and then gradually increases to its maximum value 30-40 sec after scram, a steady-state analysis at the maximum power-to-flow ratio would be conservative.

Figure 11 also shows the maximum coolant temperatures as a function of external heat flux for the conservative case of 7% power and 10% flow. Local coolant boiling (~1700°F for shutdown conditions, where the pressures are substantially lower than that at normal reactor operating conditions)

becomes a possibility for external heat fluxes greater than about 0.4×10^6 Btu/hr-ft^2. This is only slightly higher than the heat flux due to the maximum non-boiling fuel thickness under shutdown conditions. Therefore, local coolant boiling may occur if there are large temperature gradients in the coolant region adjacent to the duct wall.

In conclusion, local coolant boiling due to an external heat flux to one flat of the subassembly is not expected to occur for normal subassembly geometry. For full-power, full-flow conditions, the highest average coolant temperatures in the region next to the duct wall are about 1300°F, or 500-600°F below the local coolant boiling point, for the maximum expected heat fluxes from molten fuel. Furthermore, the duct wall is substantially melted for values of the external heat flux that can produce local coolant boiling. For reactor-shutdown conditions, the coolant temperatures are only slightly lower than the local coolant boiling point for the maximum expected heat fluxes.

2. Partially Deformed Fuel Subassembly

In this section, the coolant flow and temperature in a partially deformed fuel subassembly adjacent to an accident subassembly are studied. Two situations are considered: (1) The adjacent fuel subassembly is deformed symmetrically on all six flats, and (2) the adjacent fuel subassembly is deformed on one flat only. The situation in which all six flats of the subassembly duct are deformed is of little practical interest, but is included here to assist in understanding the situation of deformation of only one flat. In this latter case, the corners of the subassembly hex-duct are assumed to act as perfect hinges.

The deformed-subassembly geometry consisted of progressively moving one or all six flats of the duct inward. Four cases were considered: contact between duct wall and fuel pin, and additional compression of one, two, and three rows of fuel pins. Figure 12 shows the axial location of the assumed 12-in.-long deformed section, which extends from the midcore downward. The deformed section includes 2-in. sections at both ends, where the changes in duct cross section are assumed to vary linearly. Deformation of the duct wall and the pin bundle were analytically simulated by local reduction of the coolant-subchannel flow areas and gap spacings. For all cases, the corner-to-corner width of the duct flat was assumed to remain constant in spite of the deformation.

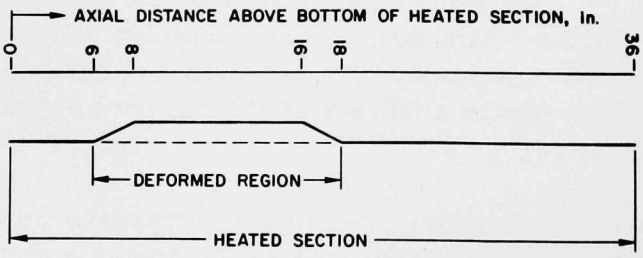

Fig. 12

Axial Variation in Flow Areas and Gap Spacings in a Deformed Subassembly. ANL Neg. No. 900-3640.

The wire-wrap spacers were represented as though they were pressed into the cladding and duct wall at the contact points, and were smeared

in the coolant subchannels between contact points. The gap spacings were reduced to 10% of the normal values to avoid excessive iterations in numerical calculations.

The Argonne modified version[23] of COBRA-III computer code was used in this study. The subchannel-analysis method of COBRA assumes that the coolant in a subchannel at any axial location is uniform and that it can be represented by an average value. This might not be the case when the pin bundle is deformed and there is a high external heat flux to the duct wall, since severe temperature gradients might exist within the coolant subchannels adjacent to the heated surface. This, together with the cladding temperatures, is discussed in Sec. 3 below. All the coolant temperatures discussed in this section refer to the average values.

Deformation of the subassembly duct walls and the fuel-pin bundle may change the pressure-drop characteristics of the pin bundle and cause a significant reduction in the inlet coolant flow to the subassembly. In the present study, pressure drop across the subassembly was assumed to remain constant by adjusting the inlet flow rate.

Although the use of the wire-wrap flow-sweeping model would give more realistic results in situations involving a high external heat flux to the subassembly duct wall, the difficulty in characterizing the action of the wire-wrap spacers in the deformed region led to the use of an effective turbulent-mixing parameter instead. The results thus obtained are more conservative; i.e., the coolant temperatures are higher next to the wall than actually expected to occur.

The nominal conditions and geometry used in the calculations correspond to those of the FTR-rated-core high-power subassembly at beginning of life and are listed in Table III, which differs from Table II because of specific interest[24] in conditions slightly different from those tabulated in Ref. 20.

TABLE III. Operating Conditions and Geometry for External Heat-flux Analysis; Partially Deformed Subassembly

Pin OD, in.	0.23
Pin-to-pin triangular pitch, in.	0.286
Heated length, in.	36
Average fuel-pin linear power, kW/ft	11.06
Axial power peaking factor (chopped cosine)	1.24
Nominal inlet mass velocity, 10^6 $lb_m/hr\text{-}ft^2$	4.432
Coolant inlet temperature, °F	792
Nominal core ΔT, °F	328 (19-pin) 355 (37-pin) 366 (61-pin) 395 (217-pin)
Pressure drop across subassembly, psi	107

For external heat flux caused by the deposit of molten fuel, the heat flux is assumed to uniformly cover the deformed 12-in. axial length over the flat (or flats in the case of symmetrical deformations).

a. Fuel Subassembly with Symmetric Deformation of Six Flats. Due to symmetry, only a 1/12th section of the fuel subassembly with symmetric deformation of all six flats needed to be analyzed. The subchannel geometries of a 217-pin subassembly for normal geometry, wall/pin contact, one row compressed, two rows compressed, and three rows compressed are shown in Figs. 13-17, respectively.

Figure 18 shows the effect of the deformation of the subassembly duct walls and the fuel-pin bundle on the inlet coolant flow rate to the subassembly. The change in inlet flow rate to maintain a constant pressure drop across the subassembly and its effect on coolant temperature distribution were examined for various cases. For wall/pin contact, the inlet flow rate was assumed to remain constant because the decrease was only about 1%.

(1) Results for Wall/Pin Contact. The subchannel geometry for the case in which duct walls touch the outer row of fuel pins is shown in Fig. 14. For the reduction of the wall/pin-gap spacing to 10% of its normal

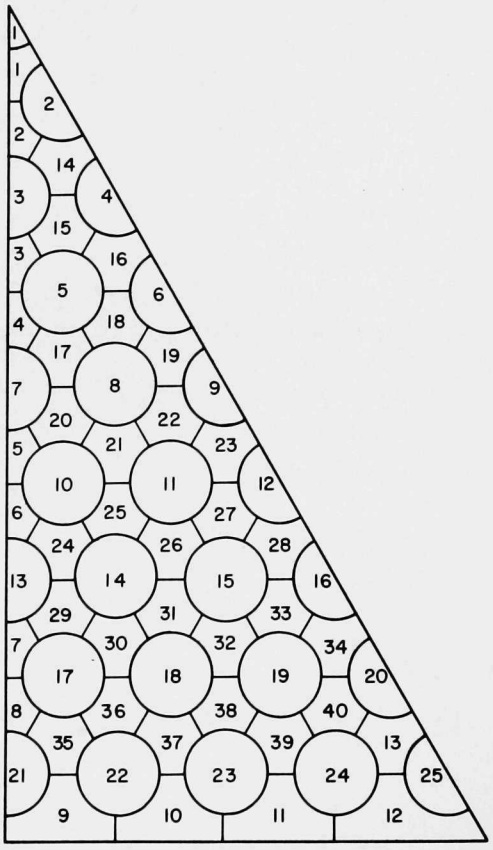

Fig. 13. Model of 1/12th Section of a 217-pin Bundle; Normal Geometry

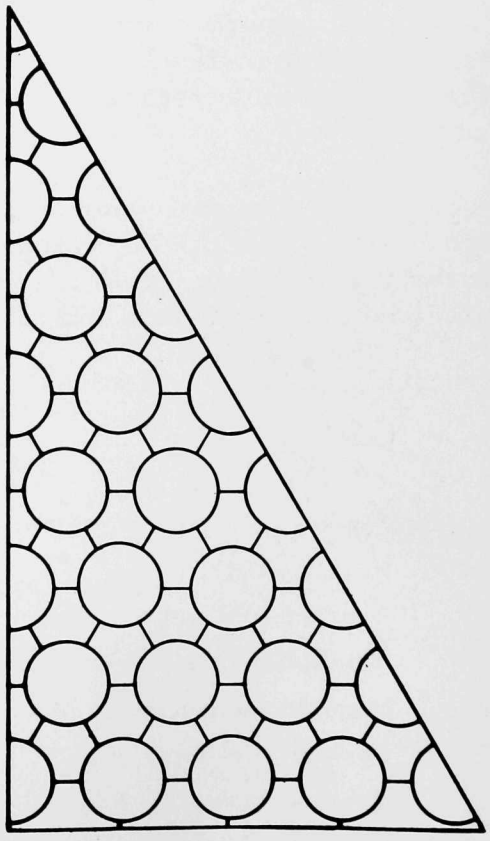

Fig. 14. Model of 1/12th Section of a 217-pin Bundle; Wall/Pin Contact

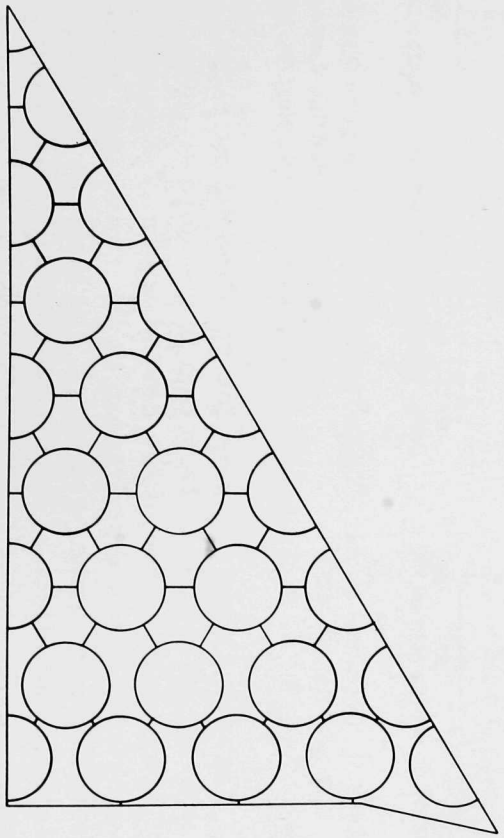

Fig. 15. Model of 1/12th Section of a 217-pin Bundle; One Row Compressed. ANL Neg. No. 900-3595.

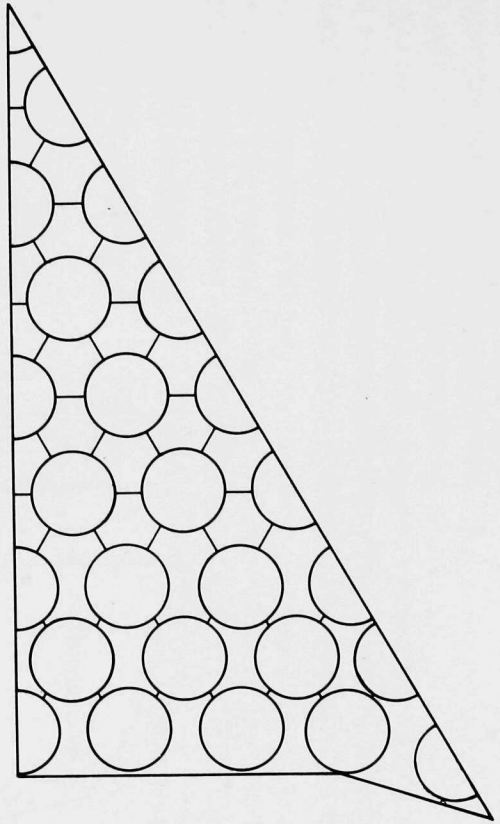

Fig. 16. Model of 1/12th Section of a 217-pin Bundle; Two Rows Compressed

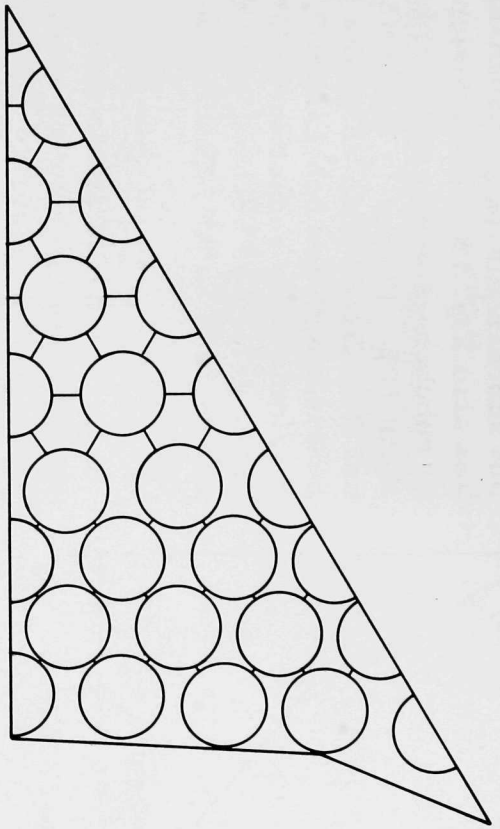

Fig. 17. Model of 1/12th Section of a 217-pin Bundle; Three Rows Compressed

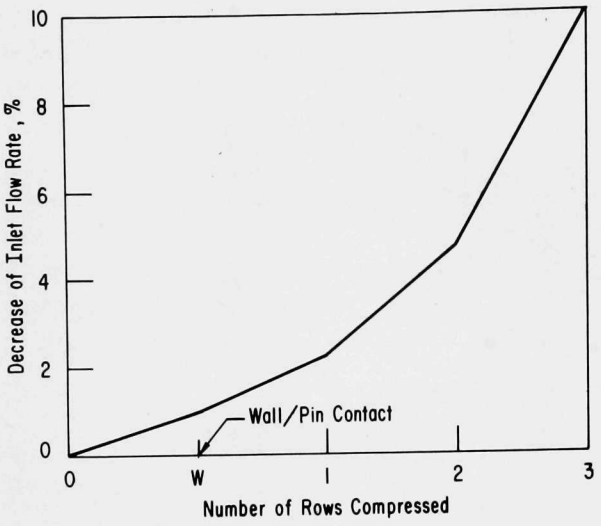

Fig. 18. Change in Inlet Flow Rate of the 217-pin Bundle due to Deformation

value, the flow area of the outer coolant subchannels (e.g., Subchannel 9; see also Fig. 13 for the designation of subchannel numbers) is reduced to about 60%. Figure 19 shows the coolant flow distribution along the 36-in. heated length for Subchannel 9. A maximum flow reduction of 70% occurs in the deformed section, and the flow recovers to about 94% of its normal value.

Figure 20 shows the coolant-temperature distribution along the 36-in. heated length for Subchannel 9 when there is no heat flux external to the subassembly. The maximum coolant temperature in the deformed region is about 85°F higher than the normal value. Downstream of the deformed region, the temperature increase is reduced because of mixing between adjacent subchannels. At the top of the heated section, the temperature is only about 50°F higher than the normal value.

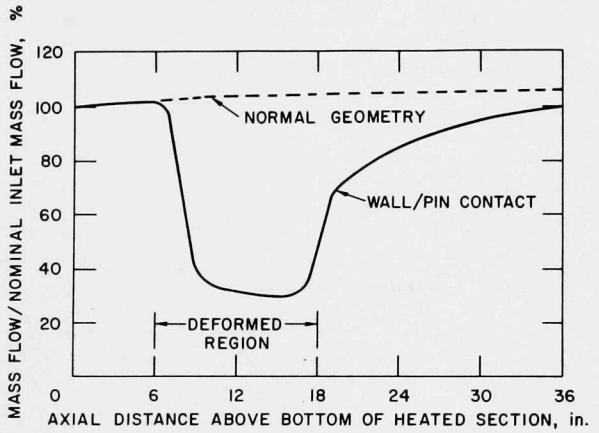

Fig. 19. Axial Flow Distribution in Subchannel 9 for Wall/Pin Contact. ANL Neg. No. 900-4052.

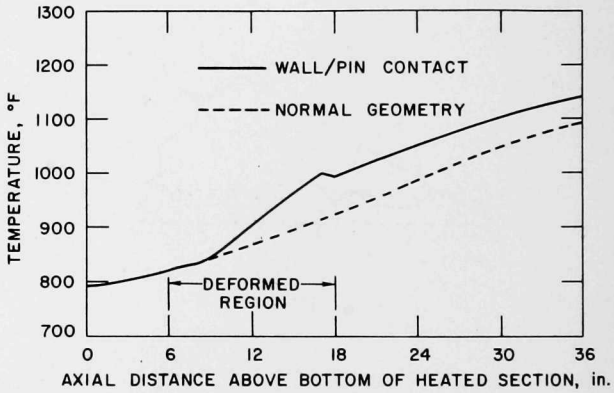

Fig. 20. Axial Coolant Temperature Distribution in Subchannel 9 for Wall/Pin Contact in the 217-pin Bundle. ANL Neg. No. 900-4046.

Figures 21 and 22 show the corresponding radial (across-flats) coolant-flow and -temperature distribution in the subassembly, respectively, at both the midcore and the top of the heated section. Except for the outer coolant subchannels, the flow distribution in the remainder of the fuel bundle remains uniform as for normal geometry. In fact, the deformation of the duct walls counteracts the effect of normal coolant-flow streaming in the outer subchannels and actually results in a more uniform radial temperature distribution.

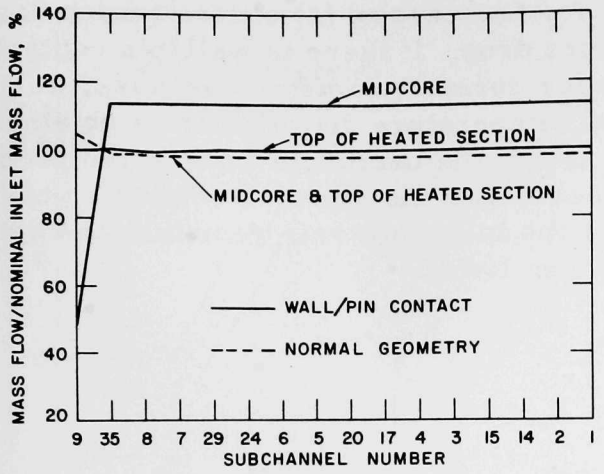

Fig. 21. Radial Flow Distribution for Wall/Pin Contact

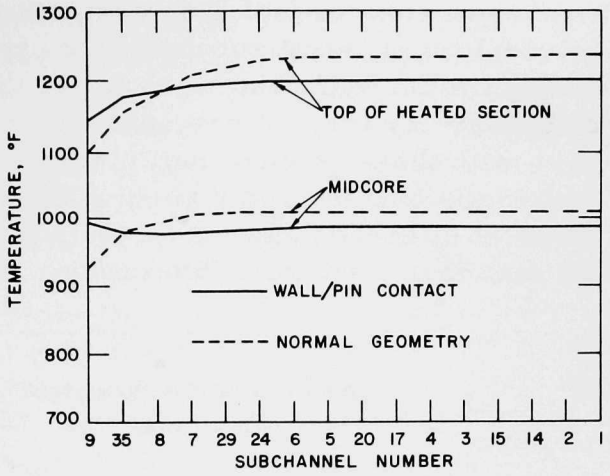

Fig. 22. Radial Coolant-temperature Distribution for Wall/Pin Contact in the 217-pin Bundle

For a high external heat flux applied over the length of the deformed region on all six flats of the subassembly duct, Fig. 23 shows the maximum coolant temperature in the deformed region as a function of the external heat flux. For normal reactor operating conditions, coolant boiling in the deformed region would not be expected to occur for temperatures below about 1800°F. For realistic values of the heat flux (less than 2×10^6 Btu/hr-ft^2), the maximum coolant temperatures are substantially lower than the boiling temperature. Therefore, local boiling is not expected to occur, except for unrealistically high values of heat flux (above 4×10^6 Btu/hr-ft^2), in which case a substantial fraction of the duct wall is molten.

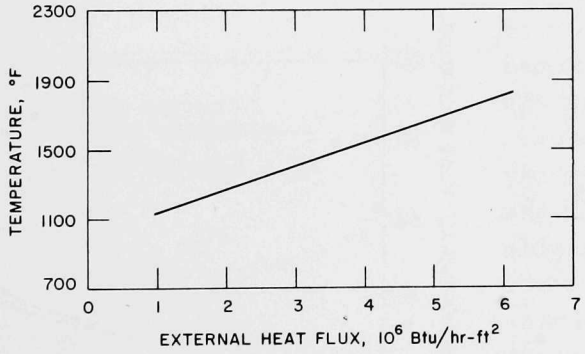

Fig. 23

Maximum Coolant Temperature in the Deformed Region due to an External Heat Flux for Wall/Pin Contact

(2) Results for Compression of Fuel Pins. The subchannel geometries for compression of one, two, and three rows of fuel pins are shown in Figs. 15-17, respectively. For these cases, note that some of the subchannels have been combined compared to the normal geometry (e.g., Subchannels 9 and 35, 10 and 37, 11 and 39, and 12 and 13). This was done to alleviate excessive numerical-iteration problems that were encountered when the reduction in subchannel area was very large (>75%).

For no external heat flux to the subassembly, Fig. 24 shows the maximum coolant temperatures in the bundle as a function of the

number of rows of fuel pins compressed for two cases: (a) constant inlet flow rate and (b) constant subassembly pressure drop. If there is wall/pin contact, the maximum temperature is lower than for normal geometry, because, as discussed earlier, a more uniform radial temperature distribution is obtained. Even with three rows of fuel pins compressed, the maximum coolant temperature in the bundle is only about 1340°F, well below the expected saturation temperature of the coolant. If we assume that the inlet flow rate remains constant, the maximum coolant temperatures are even lower.

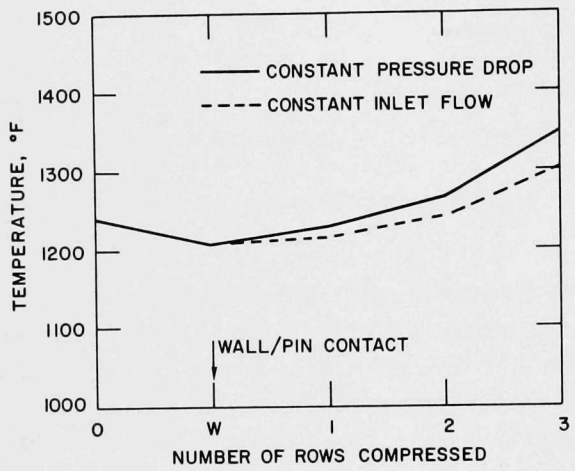

Fig. 24

Maximum Coolant Temperatures in the 217-pin Bundle due to Deformation for Constant Inlet Flow and Constant Subassembly Pressure Drop. ANL Neg. No. 900-4044.

Figure 25 shows the minimum subchannel flow rate in the deformed region as a function of the number of rows of fuel pins compressed. For the cases studied, the minimum subchannel flow rate in the deformed region increases as the number of rows compressed increases. This occurs because there are two competing factors that determine the minimum subchannel flow rate in the deformed region. As the number of rows compressed increases, the total inlet flow to the subassembly decreases, as shown in Fig. 18. On the other hand, less total area is available for coolant flow as more rows of pins are compressed; as a result, a larger fraction of the total flow is forced through the subchannel having the reduced area. The latter effect is dominant when up to three rows of fuel pins are compressed.

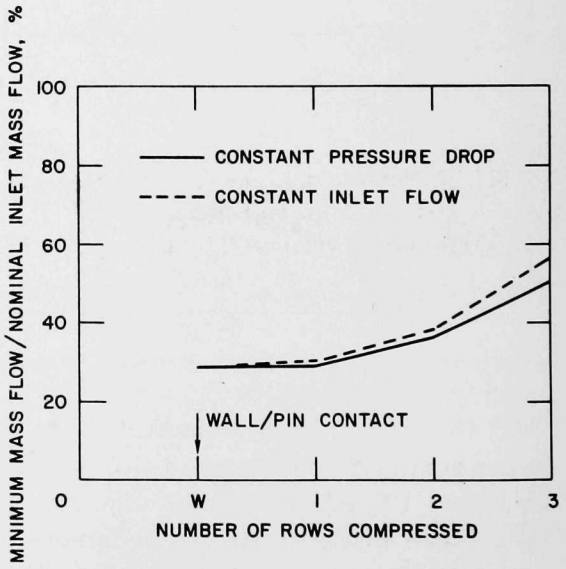

Fig. 25. Minimum Subchannel Flow (Subchannel 9) in the 217-pin Bundle due to Deformation for Constant Inlet Flow and Constant Subassembly Pressure Drop. ANL Neg. No. 900-4054.

To illustrate this point, Fig. 26 shows the minimum subchannel flow rate for three cases of fuel-pin compression. For example, the minimum flow rate for a subchannel with 40% of its normal area is 34% of its normal

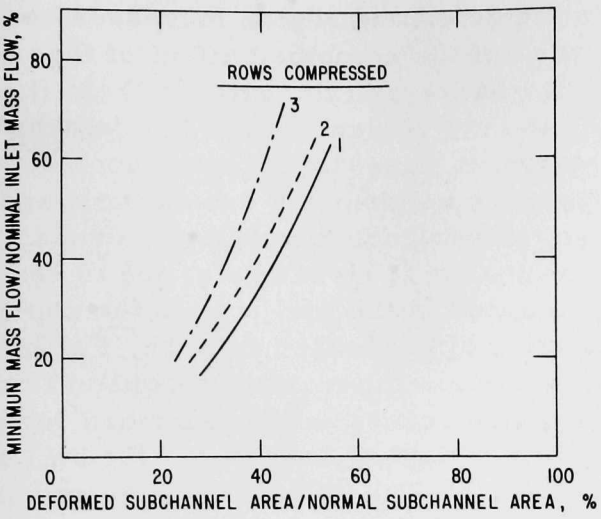

Fig. 26. Minimum Subchannel Flow as a Function of Flow Area and Number of Rows of Fuel Pins Compressed

value when one row of fuel pins is compressed, 40% when two rows are compressed, and 56% with three rows compressed. As more and more rows of fuel pins are compressed, the overall subassembly pressure drop would be expected to increase until it eventually dominates and the inlet flow rate to the subassembly is substantially reduced, so that the minimum subchannel flow rate starts to decrease. Compression of more than three rows of fuel pins has not been analyzed.

For a high external heat flux to the subassembly duct applied over the length of the deformed region, Fig. 27 shows the maximum coolant temperatures in the deformed region as a function of the external heat flux. The highest coolant temperatures are obtained when one row of fuel pins is compressed, because, as discussed above, the minimum subchannel flow rate increases as the number of rows of fuel pins compressed increases from one to three. Because of the combined effects of reduced total flow and the continued addition of fuel-pin heat flux above the deformed region, the maximum coolant temperatures in the 12-in. deformed region (see Fig. 27) might be different from those occurring in the 36-in. heated region. The maximum coolant temperature in the 36-in. bundle is shown in Fig. 28.

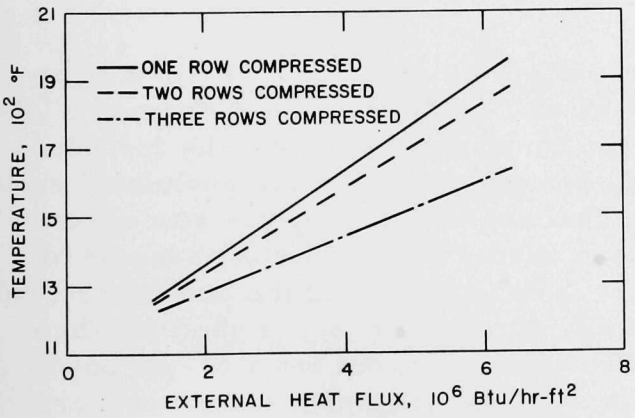

Fig. 27. Maximum Coolant Temperatures in the Deformed Region of the 217-pin Bundle due to External Heat Flux and for Various Degrees of Deformation. ANL Neg. No. 900-3645.

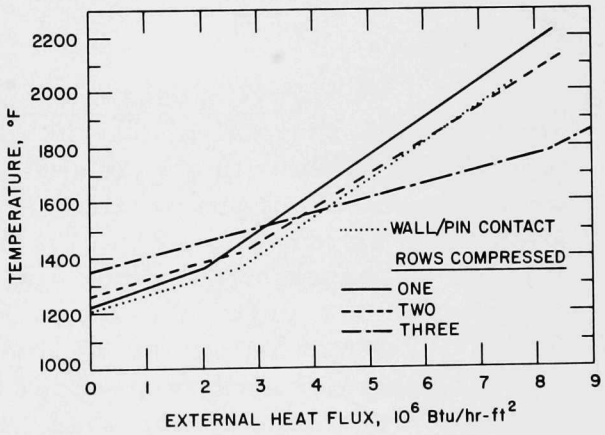

Fig. 28. Maximum Coolant Temperatures in the 217-pin Bundle due to External Heat Flux and for Various Degrees of Deformation

Figure 29 shows the axial coolant-temperature distribution along the heated section for the combined Subchannels 9 and 35 for one row of fuel pins compressed under various situations. The coolant temperature

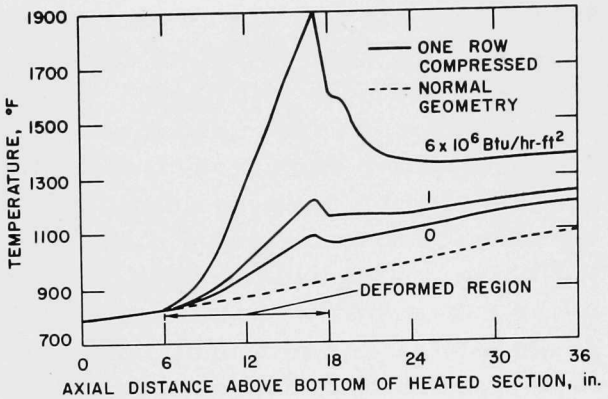

Fig. 29. Axial Coolant Temperature Distribution in Combined Subchannels 9 and 35 for One Row Compressed and with an External Heat Flux

in the deformed region increases because of the combined effect of the deformation and the external heat flux. As the hot coolant leaves the deformed region, it mixes with cooler coolant from the neighboring subchannels and the temperature immediately drops. Eventually, it rises again, due to heat generated in the fuel pins in the upper portion of the heated section. For high heat fluxes, the maximum coolant temperature occurs in the deformed region, whereas for low heat fluxes (below 1 x 10^6 Btu/hr-ft^2), it occurs at the end of the heated section.

In conclusion, the results for the partially deformed subassembly indicate that local coolant boiling (1800-1900°F for normal reactor operating conditions) is not expected to occur for external heat fluxes up to 2 x 10^6 Btu/hr-ft^2. When local coolant boiling does occur, the external heat flux is at such a level that a substantial fraction of the duct wall is molten. These results for the partially deformed bundle are quite conservative in that all six flats of the subassembly duct are deformed and the external heat flux is applied to all six flats. This case might be more reasonable if the subassembly were surrounded by six accident subassemblies. In the more realistic case of a single accident subassembly surrounded by six adjacent subassemblies, only one flat of an adjacent subassembly would be expected to be severely deformed and/or subjected to high external heat flux. This case is discussed in Sec. b below.

b. Fuel Subassembly with Deformation of One Flat. In the previous section, thermal-hydraulic analyses of a symmetrically deformed FTR-type subassembly with all six sides of the duct pressed against the fuel pins were presented. In this section, results are presented for the postulated situation in which only one side of the duct, that nearest the rupture site of an accident subassembly, is deformed. Each corner of the duct is assumed to act as a perfect hinge. Due to symmetry, a half-section of the bundle, instead of the 1/12th section for the symmetrically deformed case, is used for the present analysis. Figure 30 shows the subchannel layout for a 61-pin bundle with one row of pins compressed. Because of the excessive computer-core storage and running time required, only bundles of 19, 37, and 61 pins were investigated. Symmetric deformation of all six sides of these pin bundles was also studied, so that by comparing these results and those for the symmetrically deformed 217-pin bundle, one might be able to predict the effects of a postulated one-sided deformation of a subassembly duct on coolant temperatures within a 217-pin bundle.

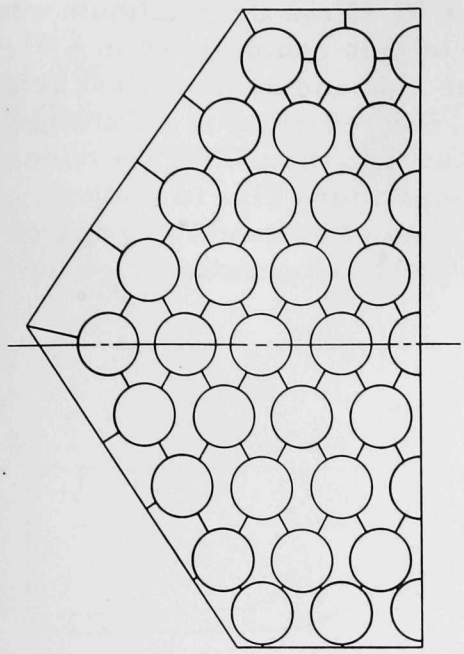

Fig. 30. Model of Half-section of a 61-pin Bundle Used for Calculations with One Row of Pins Compressed. ANL Neg. No. 900-3641.

(1) No External Heat Flux over Deformed Subassembly Duct. Axial coolant flow in subchannels immediately adjacent to the deformed flat decreases gradually in the deformed region and reaches a minimum near the top of the deformed region before it starts recovering. Figure 31 shows the minimum subchannel flow rate as a function of the number of rows of pins compressed in 19-, 37-, and 61-pin bundles. Except when the duct wall moves into contact with the first row of pins (wall/pin contact), the maximum reduction in subchannel flow is about 80%, irrespective of the magnitude of displacement or the bundle size. The maximum coolant temperature in each bundle for various displacements is shown in Fig. 32. Coolant temperature increases as more rows of pins are compressed, but it decreases somewhat as bundle size increases. For the cases studied, the maximum coolant temperature is far below the coolant saturation temperature which is in the range from 1800 to 1900°F.

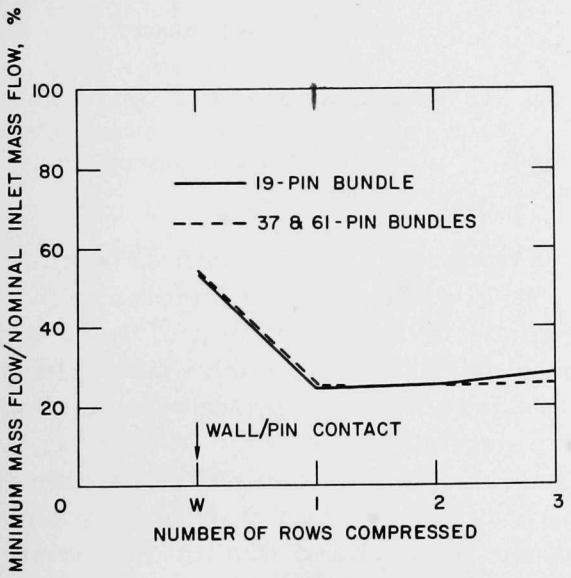

Fig. 31. Minimum Subchannel Flow Rate due to Displacement of One Side of Duct with Hinged Corners. ANL Neg. No. 900-4048.

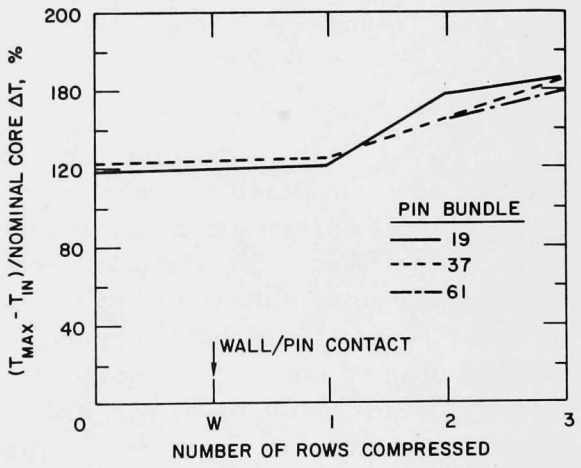

Fig. 32. Normalized Maximum Coolant Temperature Rise due to Displacement of One Side of Duct with Hinged Corners. ANL Neg. No. 900-4050.

As discussed before, the minimum subchannel flow in a symmetrically deformed subassembly becomes larger as more rows of pins are compressed. The effect of local flow-area reduction due to the compression of fuel pins is more significant than the inlet flow reduction resulting from

an increased subassembly pressure drop. Figure 33 shows the minimum subchannel flow as a function of the number of rows of pins compressed in a 61-pin bundle for both cases, i.e., deformation of one side and symmetrical deformation of six sides. Except for wall/pin contact, the reduction in subchannel flow is much larger in the one-side-deformed case than that in the six-sides-deformed case. In Fig. 34, maximum coolant-temperature rise is plotted against the bundle size for symmetrical compression of one and two rows of pins. In both cases, the normalized maximum coolant-temperature rise decreases as the bundle size increases.

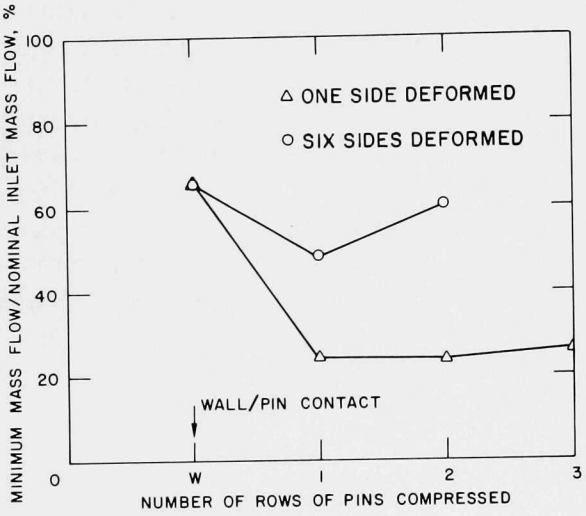

Fig. 33. Minimum Subchannel Flow Rate in a Deformed 61-pin Bundle. ANL Neg. No. 900-3639 Rev. 1.

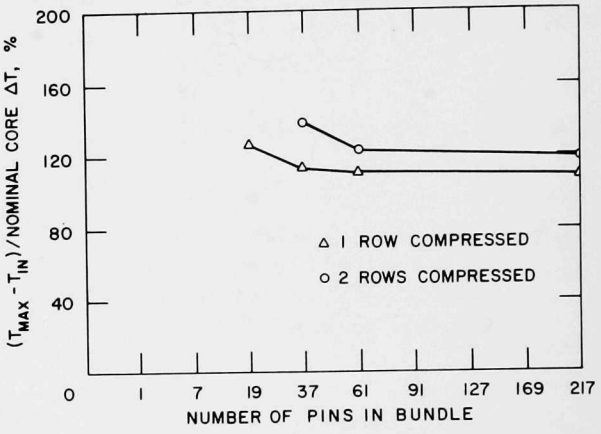

Fig. 34. Normalized Maximum Coolant Temperature Rise in Various Symmetrically Deformed Bundles with Constant Subassembly Pressure Drop

Results for various cases with 37-, 61-, and 217-pin bundles are combined and shown in Fig. 35. For the smaller bundles with symmetrical deformation, analyses were made for compression of up to two rows of fuel pins. For deformation of one side of the duct such that perturbations to the total subassembly flow area are less severe, compression of up to three rows of pins was investigated. It is evident from Fig. 35 that (a) for a given size of bundle, the normalized maximum coolant temperature rise is larger for deformation of one side of the subassembly duct than for six sides; (b) as more rows of pins are compressed, the normalized maximum coolant temperature rise also becomes larger; (c) for both one and six sides deformed, the normalized maximum coolant-temperature rise is smaller as the bundle size becomes larger. By comparing these results, one can predict the effect of deformation of one side of the 217-pin subassembly. It is concluded that the maximum coolant-temperature rise for this accident situation is between 550 and 630°F (corresponding to 140 and 160% of the nominal core temperature rise), which is significantly below the coolant saturation temperature.

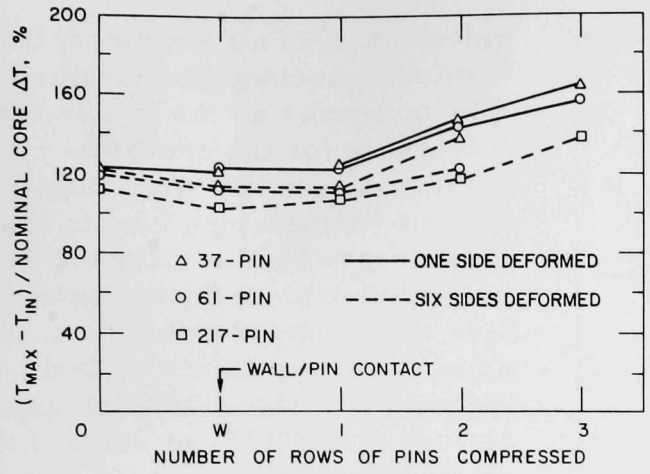

Fig. 35

Normalized Maximum Coolant Temperature in Various Deformed Bundles and for Different Magnitude of Deformations. ANL Neg. No. 900-3434 Rev. 1.

(2) External Heat Flux over Deformed Subassembly Duct. If molten fuel is deposited on the outer surface of a partially deformed subassembly duct, the external heat flux, combined with the effects of reduced subchannel coolant flow due to deformation, may result in local overheating of coolant and/or cladding. Figure 36 shows the maximum coolant temperature in the deformed region of the 61-pin bundle with an external heat flux over the bottom side of the subassembly duct (see Fig. 30). Compression of two rows of pins results in a slightly higher maximum coolant temperature than if only one row were compressed. The minimum subchannel flow is almost the same if one, two, or three rows of pins are compressed, as shown in Fig. 33. The maximum coolant temperature is therefore expected to be about the same, irrespective of the magnitude of displacement, and is expected to depend mainly upon the external heat flux. For instance, the predicted temperature difference caused by the compression of one and two rows of pins is less than 50°F, as shown in Fig. 36. Thus, for all values of heat flux below about 2 x 10^6 Btu/hr-ft^2, the maximum coolant temperature (~1450°F) for compression of up to three rows of pins in the 61-pin bundle is far below boiling (1800-1900°F).

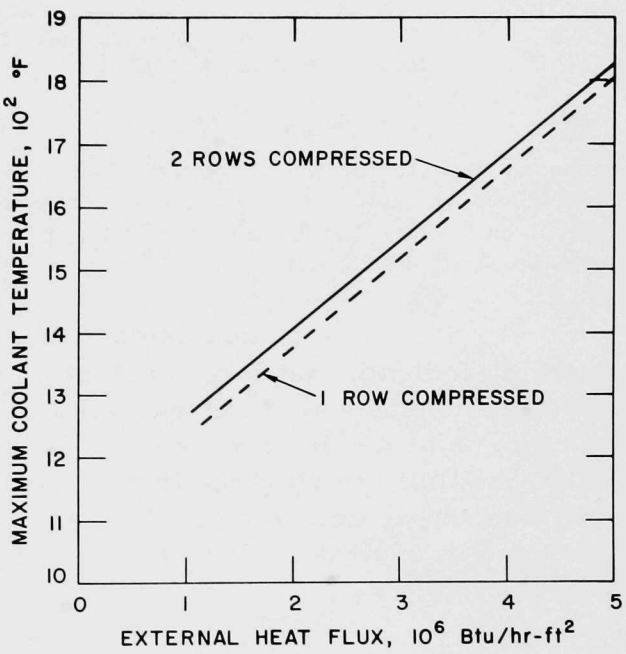

Fig. 36. Maximum Coolant Temperature in a One-side-deformed 61-pin Bundle with an External Heat Flux. ANL Neg. No. 900-3635.

Figure 37 shows, as a function of pin-bundle size, the normalized maximum coolant temperature rise when one row of pins is compressed and the external heat flux is 2.5 x 10^6 Btu/hr-ft^2. For the symmetrical

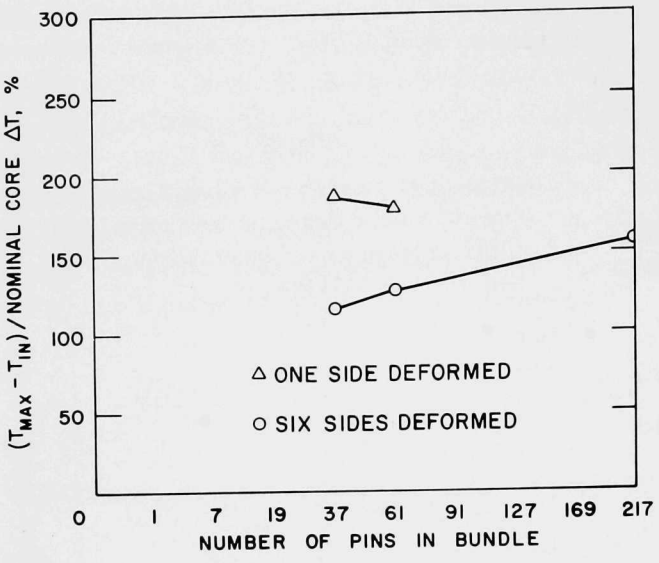

Fig. 37

Normalized Maximum Coolant Temperature Rise in Various Deformed Bundles with One Row of Pins Compressed and with an External Heat Flux of 2.5 x 10^6 Btu/hr-ft^2. ANL Neg. No. 900-3642 Rev. 1.

deformation of all six sides, the maximum coolant-temperature rise increases as the bundle size increases; for the one-side-deformed case, the maximum coolant-temperature rise is lower for a larger bundle. For the 217-pin bundle with deformation of one side of the subassembly duct, the normalized maximum coolant-temperature rise is expected to be less than 800°F, or 200% of the nominal core temperature rise, as can be seen from the results of the 37- and 61-pin bundles. Compression of more than one row of pins will result in a slightly higher maximum coolant temperature, but even in that case, no boiling is expected to occur for a heat flux less than 2.0 x 10^6 Btu/hr-ft^2.

In conclusion, the results for the partially deformed subassembly indicate that local coolant boiling (1800-1900°F for normal reactor operating conditions) is not expected to occur, even for values of the external heat flux up to 2 x 10^6 Btu/hr-ft^2. External heat fluxes that produce local coolant boiling are so large that a substantial fraction of the wall is molten. Even a severely deformed fuel subassembly subjected to high heat fluxes (produced by molten fuel) will not result in rapid failure propagation caused by coolant voiding.

3. Temperature Gradient in a Compressed Subchannel Adjacent to a Heated Wall

The coolant-subchannel temperatures predicted by COBRA represent average values as mentioned previously, and severe temperature gradients might exist within the subchannel when the pin bundle is deformed and there is a significant external heat flux to the subassembly duct. To investigate if local coolant boiling is possible for this situation, a more detailed model of a typical coolant subchannel was set up for the case in which one row of pins is compressed. As discussed earlier, this resulted in the lowest subchannel flow rate and the highest average coolant temperatures.

a. Description of Model. In Fig. 38, it is assumed that pins No. 2 and 3 contact the inside surface of the subassembly duct and that pin No. 1 contacts the other two pins. This assumption, which differs from that taken for the COBRA geometry (i.e., the gap spacing was reduced to 10% of its normal value), was made in order to estimate the maximum cladding and fuel

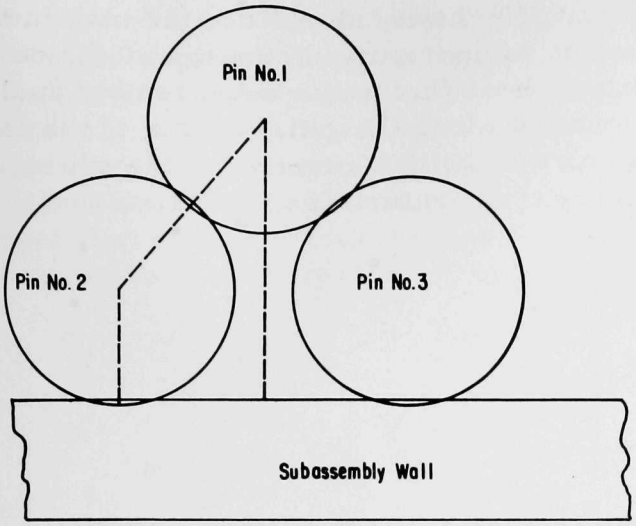

Fig. 38. Schematic of Fuel Pins and Duct Wall in a Deformed Subassembly. ANL Neg. No. 900-3605.

temperatures in the deformed pin bundle. The area of contact between the pins and the subassembly duct wall was arbitrarily assumed to extend through an angle of 10°. In estimating the free flow area for the coolant subchannel, the presence of the wire-wrap spacer was considered, but the thermal-conduction path through the wire wrap was not included in the analysis.

To simplify the nodal representation of the geometry in Fig. 38, an equivalent cylindrical geometry was used, as shown in Fig. 39. The model includes only pin No. 2 and the associated coolant region; both pin No. 1 and the subassembly wall were simulated as external heat fluxes at the boundaries of the model. The coolant flow area of the equivalent geometry is the same as in the original configuration. The 12-in. axial length of the deformed section was divided into six axial layers, resulting in a total of 720 nodes.

Fig. 39

Calculational Model for the Study of Temperature Gradient in a Compressed Subchannel Adjacent to a Heated Wall. ANL Neg. No. 900-3634.

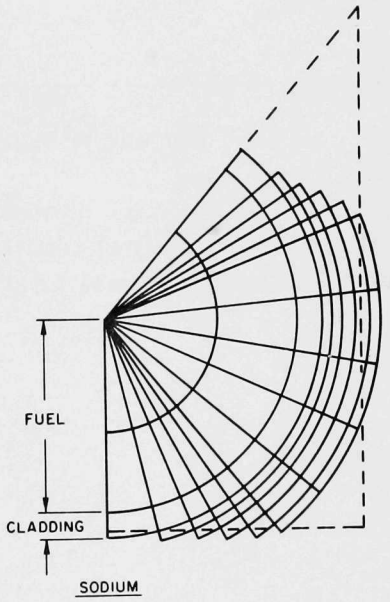

A modified version of the THTB[25] general-purpose heat-transfer code was used for the analysis. An average coolant flow rate in the subchannel was assumed, based on the COBRA results of the previous section. No mass exchange between coolant nodes occurred, and the heat transfer between coolant nodes was determined by the heat-transfer coefficients at the interfaces. These interfacial heat-transfer coefficients were approximated on the basis of equivalent thermal-conduction paths within the coolant region.

b. Analytical Results. Figure 40 shows the ratio of the maximum coolant temperature to the average coolant temperature at the top of the deformed section as a function of the external heat flux to the subassembly duct. This ratio was found to be essentially constant along the entire length of the deformed section. By use of these ratios and the COBRA results for the average coolant temperature, the maximum coolant temperatures can be calculated.

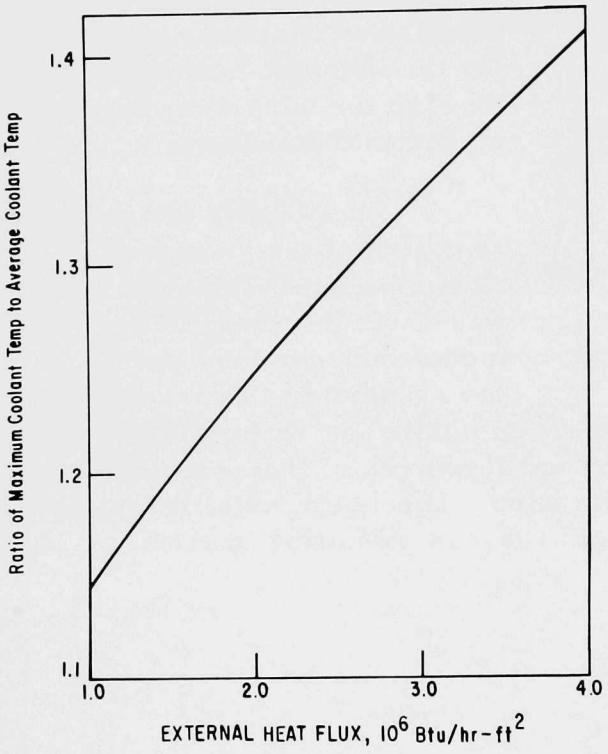

Fig. 40

Ratio of Maximum Coolant Temperature to Average Coolant Temperature as a Function of External Heat Flux in a Compressed Subchannel. ANL Neg. No. 900-3600 Rev. 1.

Figure 41 shows the ratios of the maximum cladding temperature and the maximum fuel temperature to the maximum coolant temperature as a function of the external heat flux to the subassembly duct.

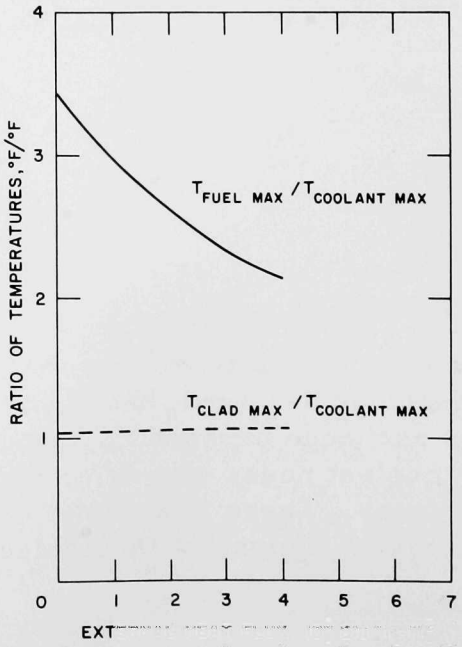

Fig. 41

Ratio of Temperatures as a Function of External Heat Flux in a Compressed Subchannel

The results are summarized in Fig. 42, which shows the maximum coolant and cladding temperatures as functions of the external heat flux to the subassembly duct. For reasonable values of the external heat flux (up to 2 x 10^6 Btu/hr-ft^2), local coolant boiling would not be expected under normal operating conditions of a reactor. However, local cladding failure may occur, depending upon the criterion used for cladding failure. For values of external heat flux such that local coolant boiling or cladding failure does become a problem, a substantial fraction of the duct wall would be molten, as shown in Fig. 3.

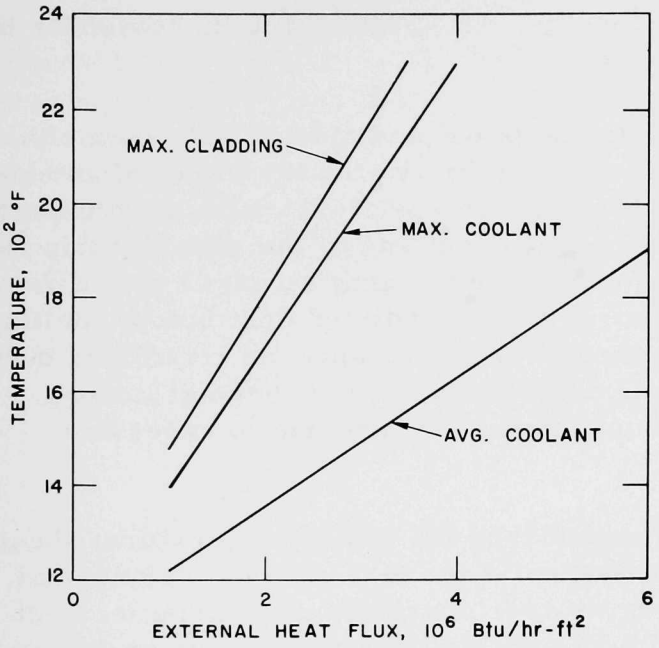

Fig. 42

Maximum Coolant and Cladding Temperatures in a Deformed Bundle with an External Heat Flux. ANL Neg. No. 900-3638.

IV. SUMMARY AND CONCLUSIONS

The response of a subassembly adjacent to an accident subassembly to certain mechanical and thermal loads has been evaluated to determine the potential for subassembly-to-subassembly failure propagation.

Previous analytical studies on the response of an adjacent subassembly duct to external pressure pulses were reviewed and summarized. Large differences in the results were found because of differences in both the analytical models and the assumed parameters. The significant uncertainties in the analyses were identified and discussed.

The effect of certain thermal loadings on the adjacent subassembly was considered in two parts. The first part investigated the effect of an external heat flux on duct melting and thermal stresses. The maximum expected heat fluxes due to molten fuel deposited on the outside of the subassembly did not result in duct melting. However, excessive thermal stresses may cause deformation and/or mechanical failure of an unirradiated duct before melting occurs. Based on the limited experimental data available, an irradiated duct seems to have a significantly stronger resistance against thermal loading, and duct melting might occur before mechanical failure due to excessive thermal stresses.

The second part of the study considered the effect of an external heat flux on the coolant-temperature distribution in the fuel bundle. For normal subassembly geometry and full-power reactor operating conditions, no coolant boiling is predicted for the maximum expected heat fluxes due to molten fuel deposited outside the subassembly. Also, the heat flux required to produce coolant boiling is so high that a major fraction of the duct wall would already be molten. For reactor-shutdown conditions, the heat flux required to produce coolant boiling is still higher than the maximum expected heat fluxes due to molten fuel, although the margin to reach coolant saturation point is smaller. For the deformed subassembly geometry (up to three rows of fuel pins compressed), the conclusions are the same as for the normal subassembly geometry. A detailed model of the coolant region between the duct wall and the compressed fuel pins shows that the maximum coolant temperature can be several hundred degrees higher than the average temperature, but coolant boiling would still not be expected to occur until a substantial fraction of the duct wall is melted.

In conclusion, rapid fuel-failure propagation to several subassemblies adjacent to an accident subassembly in which molten fuel is generated is not expected to occur at normal power for a wide range of thermal loadings postulated in this report. Local failure of the adjacent subassembly duct wall from excessive thermal stresses might occur, but the leakage flow out of the subassembly is not expected to result in excessive local coolant temperature producing coolant voiding, if a concurrent heat flux is not imposed by the accident

subassembly. Even a deformed subassembly seems to have sufficient cooling capability to prevent rapid failure propagation caused by coolant voiding in the adjacent subassembly.

Additional analytical and experimental effort is needed to assess all aspects of subassembly-to-subassembly failure propagation. For example, effort is required to better understand the characteristics of the source terms produced by the postulated initial faults in an accident subassembly. If subassembly meltdown due to hypothetical initiating events such as an inlet blockage is considered, we need to answer the question of whether a largely plugged subassembly, in which most molten materials remain within the initial fuel boundary, can be formed in an LMFBR environment. Better understanding of the sequence of events following a local failure of the adjacent subassembly duct is necessary for the assessment of the potential for further failure propagation. The possibility of interaction between liquid sodium (from the adjacent subassembly) and molten materials (from the accident subassembly) in this case should also be investigated.

ACKNOWLEDGMENTS

We would like to thank many staff members of Argonne National Laboratory, Hanford Engineering Development Laboratory, and the Energy Research and Development Administration, who provided many helpful comments and suggestions during the preparation of this work.

In particular, we would like to recognize the contributions of the following ANL people: D. R. Pedersen, W. E. Miller, and R. D. Pierce, who provided helpful comments on the study of the subassembly meltthrough, and D. H. Lennox and M. A. Grolmes, who reviewed and commented on the report.

Finally, we would also like to acknowledge the helpful encouragement of B. D. LaMar.

REFERENCES

1. R. M. Crawford et al., *The Safety Consequences of Local Initiating Events in an LMFBR*, ANL-75-73 (Dec 1975).
2. R. M. Crawford et al., *Studies on LMFBR Subassembly Boundary Integrity*, ANL-75-27 (May 1975).
3. J. W. Hagan et al., *Safety Assurance Summary for the FFTF*, HEDL-TME 75-76 (1975).
4. L. M. McWethy, Editor, *An Analytical Evaluation of the Consequences of a Hypothetical Instantaneous Loss of Coolant Flow to a Fast Flux Test Facility Driver Fuel Assembly*, GEAP-10059 (July 1969).
5. R. J. Roark, *Formulas for Stress and Strain*, 3rd Edition, McGraw-Hill Book Co., Inc., New York (1954).
6. L. M. McWethy, P. R. Pluta, and D. B. Sherer, Editors, *Core Design Development Needs in Relation to Fuel Failure Propagation, Sodium Boiling, and Clad/Fuel Sodium Thermal Interaction*, GEAP-13639-2 (Oct 1970).
7. S. Y. Pan, Atomics International, personal communication (June 1970).
8. R. D. Coffield and P. L. Wattelet, *An Analytical Evaluation of Fuel Failure Propagation for the Fast Flux Test Facility*, WARD-AT(45-1)2171-7 (Dec 1970).
9. J. A. Swanson, *FEATS, A Computer Program for the Finite Element Thermal Stress Analysis of Plane or Axisymmetric Solids*, WANL-TME-1888 (Jan 1969).
10. *Recommended Method for Obtaining the Deflection of a Hexagonal Control Rod Duct for a Specified Pressure Loading*, MPR Associates, Inc., Washington, D.C. (Dec 1971).
11. J. C. Hesson, R. H. Sevy, and T. J. Marciniak, *Post Accident Heat Removal in LMFBRs: In-vessel Considerations*, ANL-7859 (Sept 1971).
12. *ASME Boiler and Pressure Vessel Code, Section III, Nuclear Power Plant Components* (1971).
13. Unpublished information, Hanford Engineering Development Laboratory (1971).
14. J. G. Conner and S. W. Porembka, *A Compendium of Properties and Characteristics for Selected LMFBR Cladding Material*, BMI-1900 (May 1968).
15. F. A. Comprelli et al., *Mechanical Properties of Irradiated Type-304 and Type-316 Stainless Steel in Fast Reactors*, GEAP-10062 (June 1969).
16. W. E. Miller, D. R. Pedersen, and R. D. Pierce, ANL, personal communication (June 1973).
17. A. W. Graves and I. Catton, *A Numerical Model of Heat Transfer in a Rod Bundle with Helical Wire-wrap Spacers*, ASME Paper No. 72-HT-55, presented at National Heat Transfer Conference in Denver, August 1972.
18. D. R. Pedersen et al., *Crossflow Mixing in a 91-element Wire-wrapped Bundle*, Trans. Am. Nucl. Soc., *19*, 306 (Oct 1974).
19. J. J. Lorenz et al., ANL, personal communication (Feb 1974).
20. *Fast Flux Test Facility System Design Description for Reactor System*, SDD-31, Rev. 1 (May 1972).

21. A. W. Graves, Atomics International, personal communication (Apr 1973).

22. *Fast Flux Test Facility System Design Description for Reactor System*, SDD-31, Rev. 6 (Feb 2, 1973).

23. W. W. Marr, *COBRA-3M: A Digital Computer Code for Analyzing Thermal-hydraulic Behavior in Pin Bundles*, ANL-8131 (Mar 1975).

24. R. M. Crawford, ANL, private communication (Apr 25, 1973).

25. G. L. Stephens and D. J. Campbell, *Program THTB for Analysis of General Transient Heat Transfer Systems*, Report No. R60FPD647, General Electric Co. (Apr 1961).